



# Laboratory study of plugging mechanism and seal integrity in fractured formations using a new blend of lost circulation materials

Behzad Elahifar<sup>1</sup> · Erfan Hosseini<sup>2</sup>

Received: 2 January 2022 / Accepted: 2 January 2023 / Published online: 19 January 2023  
© The Author(s) 2023

## Abstract

The problem of lost circulation occurred long during the drilling operation. Through induced and natural fractures, huge drilling fluid losses lead to higher operating expenses during the drilling. Historically, this problem was addressed with the help of the Lost Circulation Materials (LCMs). These materials are added to the drilling fluid to seal the fractures and increase fracture initiation or propagation pressure. Therefore, understanding the mechanisms of fracture sealing and the performance of the lost circulation materials is critical if the problem of lost circulation is to be mitigated effectively. Despite extensive advances in the last couple of decades, lost circulation materials used today still have disadvantages, such as damaging production zones, failing to seal large fractures, or plugging drilling tools. Here, we propose a new blend of smart expandable lost circulation material (LCM) to remotely control the expanding force and functionality of the injected LCM. This paper aimed to assess the performance of the selected LCMs (Mica, Wheat Straw, Oak Shell, and Sugarcane Bagasse Fiber or Canes) in water-based drilling fluids. The particle bridging of LCMs was investigated using particle bridging experiments in the laboratory. Moreover, we determined the particle size distribution of D50. The cell utilized in the sealing experiments had 1000- and 3000 micron fractures to mimic different size fractures in the formation. Fracture widths are predicted based on well-log data and adaptation of existing models in the desired oil field. The concentrations of LCMs in Mica, Wheat Straw, Oak Shell, and Sugarcane Bagasse Fiber (Canes) were (25, 50, and 80 ppb), (1.5, 2, 2.5 ppb), (3, 6, and 10 ppb), and (1.5, 2, 2.5 ppb), respectively. The results indicate that a combination of LCMs outperforms individual LCMs. When used individually, Oak Shells performed the highest, followed by Mica and Sugarcane Bagasse Fiber mixtures. Also, the Wheat Straw blend served the weakest lost circulation treatments. Finally, the combination applied in this investigation successfully sealed fractures up to 3 mm in diameter in the targeted oil field, which traditional LCM would be unable to do. Due to the abundance and low cost of these materials in the study area, they can be used to ensure successful plugging.

---

✉ Erfan Hosseini  
e.hosseini19@put.ac.ir

Behzad Elahifar  
behzad.elahifar@ntnu.no

<sup>1</sup> Department of Geoscience and Petroleum, Norwegian University of Science and Technology (NTNU), Trondheim, Norway

<sup>2</sup> Exploration Directorate, National Iranian Oil Company (NIOC), Tehran, Iran

## Graphical Abstract



**Keywords** Lost circulation material · Fracture propagation · Particle size distribution · Oak Shell · And particle bridging

### Abbreviations

C	Canes
ECD	Equivalent circulation density
ECSs	Engineered composite solutions
GS	Gel strength
HPA	High-pressure apparatuses
HPHT	High-pressure-high-temperature
LCM	Lost circulation material
LCM	Lost circulation materials
LPA	Low-pressure apparatuses
M	Mica
MW	Mud weight
NC	Non-controlled
OBM	Oil-based mud
OS	Oak Shell
PCF	Pound per cubic foot
PPA	Particle plugging apparatus
PPB	Pound per barrel
PPG	Pound per gallon
PSD	Particle size distribution
PV	Plastic viscosity (cp)
W	Wheat Straw
WBM	Water-based mud
YP	Yield point (lbs. /100 ft <sup>2</sup> )

### Introduction

Fluid loss into formation during drilling is one of the most challenging things to minimize or manage. Consequences include the loss of costly drilling fluid, non-productive time (NPT), and wellbore loss. In some situations, blow-outs are worse than the losses themselves. According to current reports, approximately 1.8 million barrels of drilling fluid are lost annually (Jeennakorn et al., 2017; Alsaba and Nygaard 2014). This enormous simple result of the operational difficulties encountered in the drilling industry. Natural or induced fractures commonly occur in lost circulation (AlAwad 2022; Restrepo et al., 2010). Mitigating natural fractures requires understanding the fracture's size to develop a suitable treatment, and fracture extent is difficult to evaluate (Ezeakacha et al. 2017; Cook et al., 2016). On the other hand, induced fractures can be prevented or mitigated by managing the equivalent circulation density (ECD) or strengthening the wellbore. While conventional LCM treatments are frequently employed to limit seepage and partial losses, there is no industry-wide consensus on handling extreme losses (Alsaba 2016; Ghalambor et al., 2014; Kefi et al., 2010). When evaluating the performance of LCM treatments, the volume of fluid lost is frequently

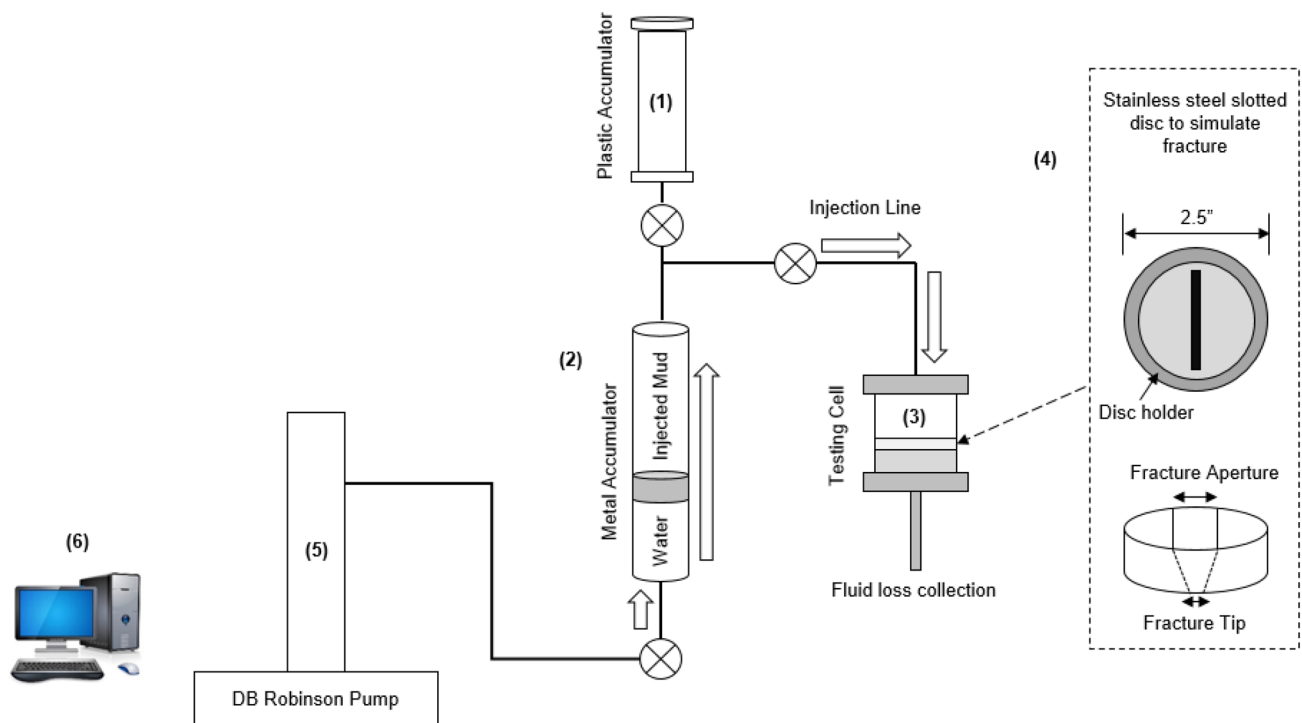


**Fig. 1** Schematic diagram of the experimental setup for particle bridging tests at high and low pressures. ((1) A plastic accumulator; used to transfer the drilling fluids, (2) A metal accumulator;

before pressurizing the fluids containing LCM treatments, (3) Testing cell, (4) Tapered disks, (5) DB Robinson Pump, (6) Computer; connected to pump for pressure versus time measurements)

considered. Fluid loss amounts during LCM treatments are commonly determined using particle plugging apparatus (PPA) and high-pressure-high-temperature (HPHT) fluid loss in conjunction with slotted/tapered disks or ceramic disks (Mansour et al. 2019; Cook et al. 2012; Kumar et al. 2010). These tests may accurately estimate the total drilling fluid lost to the formation. However, the formed seal integrity, defined as the maximum pressure at which the developed seal breaks and fluid loss resumes, is not evaluated due to the high importance of laboratory testing before field application (Arshad et al., 2014; Whitfill 2008).

AlSaba et al. (2014a; b) conducted a thorough laboratory assessment to determine the feasibility of sealing wide fractures utilizing conventional LCMs. The effectiveness of numerous LCMs to seal fractures was investigated using a variety of tapered slot sizes ranging from 2000 microns in width. Four major types of conventional LCMs with 13 different particle sizes (D50) were tested, and one new foam wedge-based LCM was tested. Two hundred tests were conducted to determine the effect of various



**Fig. 2** Types of LCM; **a** Mica. **b** Wheat Straw. **c** Oak Shell. **d** Sugar-cane Bagasse Fiber or Canes

**Table 1** Test mud formulation

Product Name	Used	Unit	Mixing Time
Bentonite	Base fluid	24 g	20 min
Water		350 cc	
XC-Polymer	Viscofier	1 g	5 min
NaOH	PH adjust	0.45 g	

**Table 2** Test mud rheology

Parameters	Quantity
$\theta_{600}$	77
$\theta_{300}$	58
$\theta_{200}$	50
$\theta_{100}$	39
$\theta_6$	20
$\theta_3$	17
$\tau_y$ (lb./100 ft <sup>2</sup> )	12.21
k	2.8
m	0.491

parameters on the overall performance of conventional and unconventional LCM. These parameters include the type of LCM used, its concentration, the tapered slot's size, particle size distribution (PSD), temperature, and injection rate. Microscopic imaging revealed that particles with rough surfaces, such as nutshells and cellulosic fiber, generate higher friction. As a result, their sealing pressures will keep rising.

AlSaba et al. (2016) conducted an experimental study to determine LCM type, concentration, particle size distribution, temperature, and LCM shape on the formed seal integrity under differential pressure and various fracture widths. They formulated and evaluated the efficiency of nine LCM blends using three common LCMs with varying sizes. In their testing, conventional LCMs could seal

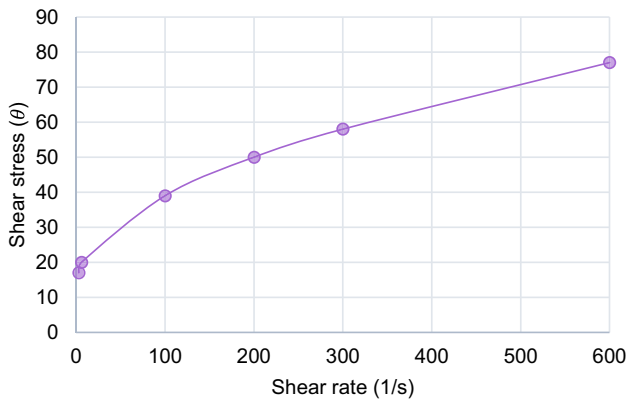


**Fig. 3** Herschel-Bulkley model for bentonite mud



**Fig. 4** a 1 mm straight cell. b 3 mm straight cell

**Table 3** Cell specification

	Length		Fracture Tip	
	in	mm	micron	mm
C1	1.97	50	1000	1
C2	1.97	50	3000	3

fractures as small as 2000 microns in diameter. Other unconventional treatments are required for fractures more than 2000 microns in diameter. They concluded that temperature does not have a substantial influence on fluid loss. Xu et al. (2017) investigated the development of a new mathematical model for assessing the drill-in fluid-loss control performance in fractured tight reservoirs by utilizing LCM. Their proposed mathematical model comprises two sub-models: plugging zone strength and fracture propagation pressure. Their modeling results showed that the particle–particle friction angle, the particle–fiber friction angle, the fiber tensile strength, the D90 degradation rate, and the friction angle between the plugging zone and the fracture surface are the main possible parameters affecting plugging zone strength. During loss control, the major

**Table 4** LCM's concentration and PSD, when used individually

	D50 (micron)	The weight percentage of total concentration, if used individually			
		Case#1	Case#2	Case#3	Case#4
Mica	440	20	14	0	0
	1540	20	20	20	0
	1840	30	26	40	50
Wheat Straw	3650	30	40	40	50
	6100	100	90	50	–
Oak Shell	1520	0	10	50	–
	740	33.3	0	0	0
Sugarcane Bagasse Fiber (Canes)	1660	33.3	50	100	0
	3700	33.3	50	0	100
	530	33.3	0	0	0
Sugarcane Bagasse Fiber (Canes)	1570	33.3	50	100	0
	3300	33.3	50	0	100

geometric parameters were the particle size distribution, the aspect ratio and initial angle of the fiber, and the plugging zone porosity.

Mansour and Taleghani (2018) introduced anionic shape memory polymers to make a new smart lost circulation material. The smart LCMs could be programmed to change shape, bridge, and expand when stimulated by a specific temperature. Their proposed smart LCM demonstrated efficient fracture sealing and provided a next-generation smart alternative for lost circulation. Their findings indicate that when the appropriate size of the smart LCM is picked, the fracture is sealed efficiently and effectively. The smart LCM's bridging and volumetric expansion properties enable it to seal big fractures and minimize or prevent fluid loss. Combining the sizes of the smart LCMs led to more effective results due to the increased packing of the particles and the bridges they make. Savari et al. (2019) present a strategy and discussion for three types of contingency particulate LCMs that were to be efficiently applied on location and demonstrated to reduce drilling non-productive time (NPT) before resorting to more difficult and time-consuming options, such as gunks/cement in highly fractured carbonate formations. Their innovative LCMs were designed around the concept of a multimodal (MM) particle-size distribution (PSD) capable of plugging a range of fracture sizes (more than 3000 microns and up to 9800 microns in one case). They defined supplementary materials (e.g., swelling polymer and reticulated foam) to improve lower-case plugging efficiency. The findings show that combining multiple engineered composite solutions (ECSs) increases the probability of working in severe/total-loss situations in naturally fractured formations.

Yang and Chen (2020) used a modified permeability plugging apparatus at room temperature to study the influence of soaking on fracture plug formation and fluid invasion volume. Their research used experimental studies and statistical approaches to investigate and quantify the impacts of fluid injection rate, plug soaking time, and soaking pressure. They concluded that a lower LCM pill injection rate resulted in a reduced fluid invasion volume following the creation of an effective fracture plug. The effects of soaking depend on the LCM combination's properties. Additionally, soaking might strengthen the plug structure by decreasing its porosity. A larger plug volume and reduced plug porosity increase plug-breaking pressure. Their findings and conclusions shed new light on identifying the optimal LCM implementation scheme with improved formation damage control. Apart from the latest advancements in this field, a significant effort remains to be made to prevent the loss of circulation of drilling fluids, which has a detrimental effect on the entire fracturing and filtration processes.

As a result of the theme, this study examines the performance of lost circulation particles in water-base mud systems. Maximum sealing pressure, optimal LCM type, concentration, particle size distribution, and fluid loss were determined in this work for both Low-Pressure Apparatuses (LPA) and High-Pressure Apparatuses (HPA).

**Fig. 5** LCM testing apparatus



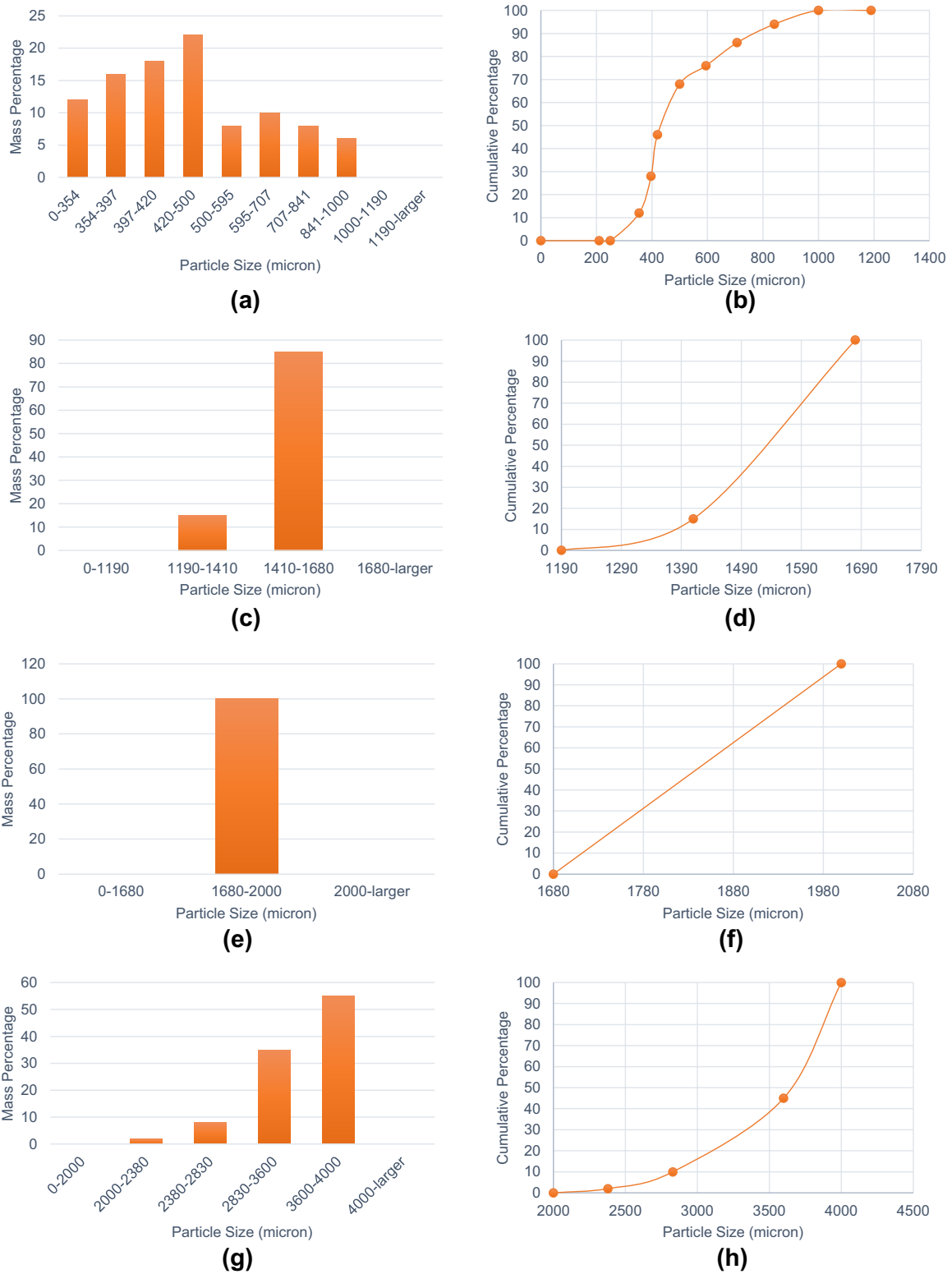


**Fig. 6** **a** Mica particle size distribution (0–1190 micron), **b** Mica cumulative particle size distribution (0–1190 micron). **c** Mica particle size distribution (1190–1680 micron). **d** Mica cumulative particle size distribution (1190–1680 micron). **e** Mica particle size distribu-

tion (1680–2000 micron). **f** Mica cumulative particle size distribution (1680–2000 micron). **g** Mica particle size distribution (2000–4000 micron). **h** Mica cumulative particle size distribution (2000–4000 micron)



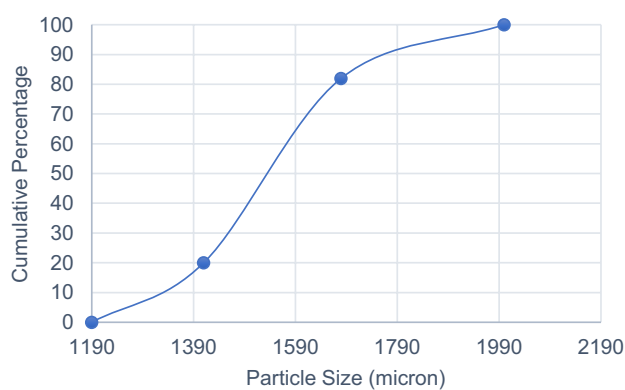
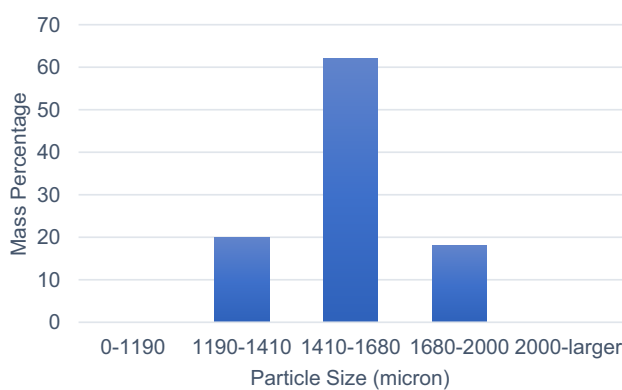
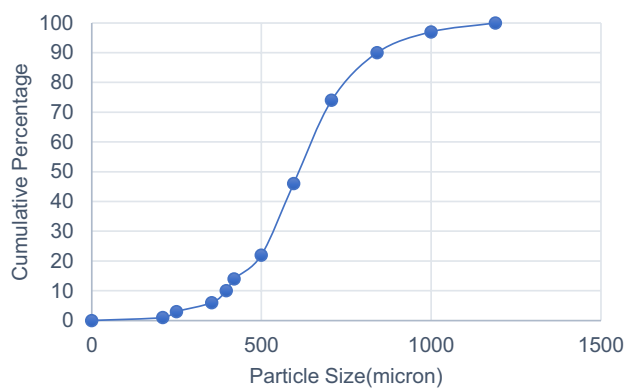
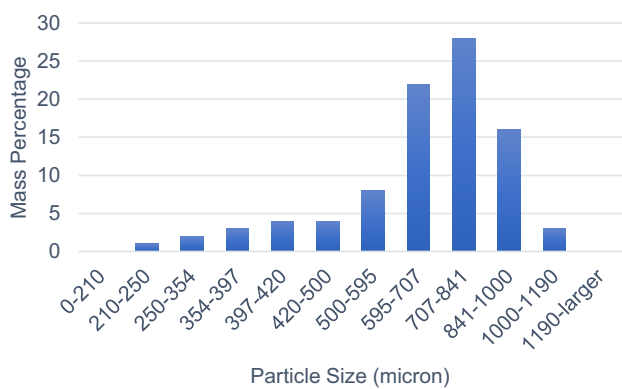
## Materials and procedures

Figure 1 depicts the system schematically. Before the experiment begins, the apparatus is a steel vessel filled with drilling fluid. An opening in the upper section of the system connects the vessel to atmospheric pressure. Water was pumped through the opening in the system at a rate of 30 ml/min when the experiment started. Water is pumped on top of the drilling fluid until the system is air-free. The vessel is closed once filled, and the pressure can be increased with the water pump. Only the opening in the lower part of the system and the particles mixed in the fluid prevent the drilling fluid from flowing out of the vessel. During the experiment, the mud's lost circulation particles built bridges on the cell, causing the vessel's pressure to rise. As the pressure builds, the particle bridges collapse; however, the pressure variation is recorded using a computer data recording system. Several bridging and collapses occur during the experiment until all of the mud from the vessel has been drained. A schematic diagram of the experimental setup for particle bridging tests at high and low pressure is shown in Fig. 1.

## Preparing and measuring the particle size distribution of lost circulation particles

Preparing the LCM and measuring particle size distribution are the first steps in the testing process. This experiment was carried out in the Petroleum University of Technology's laboratory. As shown in Fig. 2, four LCM types were used as lost circulation materials during the experiment: Mica, Wheat Straw, Oak Shell, and Sugarcane Bagasse Fiber (or Canes). The following is a list of experimental approaches for determining particle size distribution using a sieve analysis (based on weight):

1. Prepare a sample of the material.
2. Weigh the sample size to the closest 0.1 g. Please make a note of this weight and identify it as  $W_T$ .
3. Place the sieves in a pan with the largest opening on top and pour the aggregate over the top sieve.
4. Using the sieves provided in the material or project specifications, separate the material into a sequence of particle sizes.
5. The preferred way to separate the materials into the proper sizes is to utilize a mechanical sieve shaker.



**Fig. 7** **a** Wheat Straw particle size distribution (0–1190 micron). **b** Wheat Straw cumulative particle size distribution (0–1190 micron). **c** Wheat Straw particle size distribution (1190–2000 micron). **d** Wheat Straw cumulative particle size distribution (1190–2000 micron)

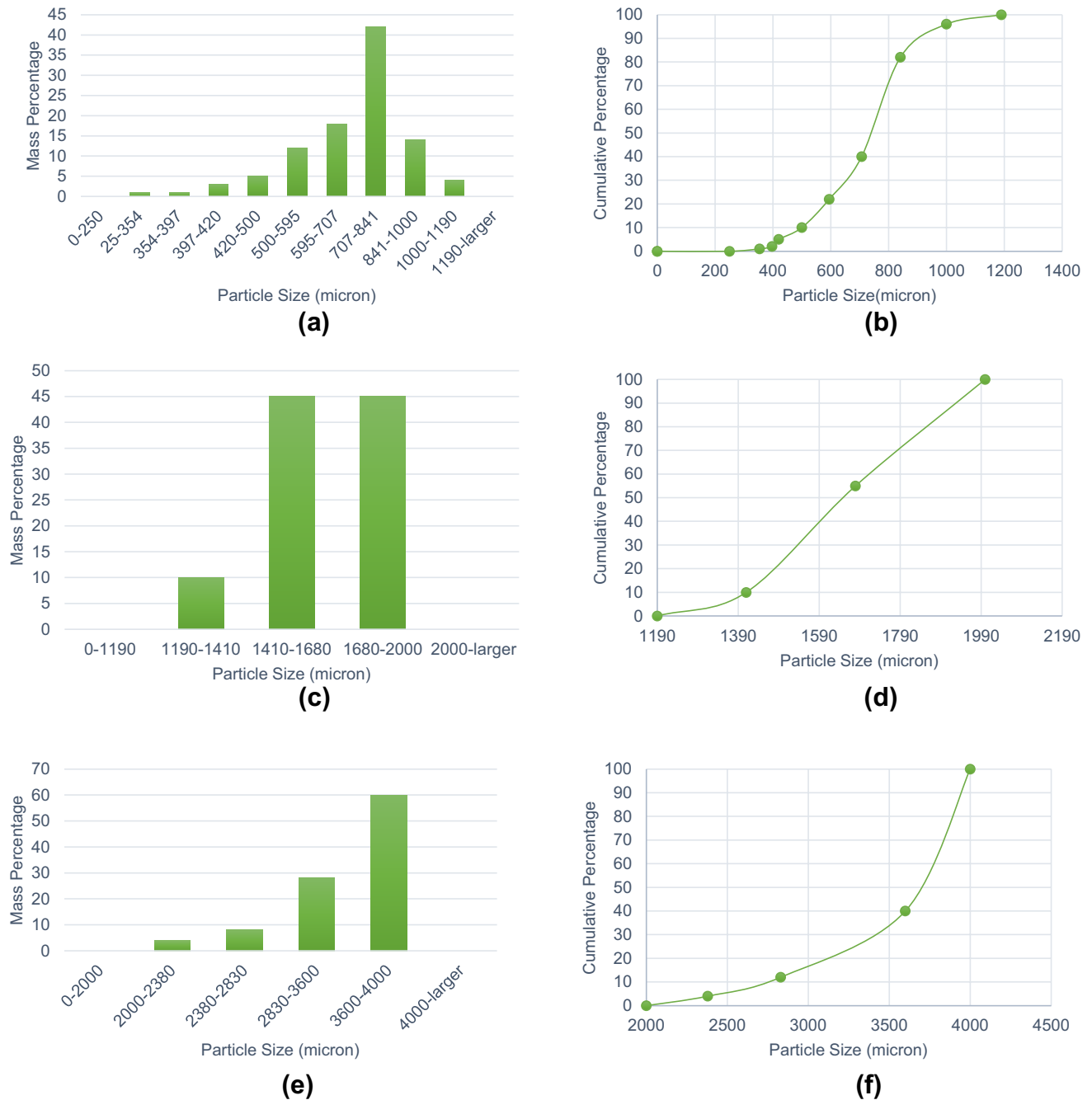


**Fig. 8** **a** Oak Shell particle size distribution (0–1190 micron). **b** Oak Shell cumulative particle size distribution (0–1190 micron). **c** Oak Shell particle size distribution (1190–2000 micron). **d** Oak Shell

cumulative particle size distribution (1190–2000 micron). **e** Oak Shell particle size distribution (2000–4000 micron). **f** Oak Shell cumulative particle size distribution (2000–4000 micron)

6. Brush particles cling to each filter and are brushed into the next lower sieve. Confirm that no material is lost.
7. Calculate and record the individual weights of aggregate retained on each filter to the closest 0.1 g.
8. Provide percentages to the closest 0.1% for each aggregate size retained on each sieve as the specification requires.

9. Calculate the percentages of weight retained between consecutive sieves using the following formula:

$$W = \left( \frac{X_1}{W_T} \right) \times 100 \quad (1)$$



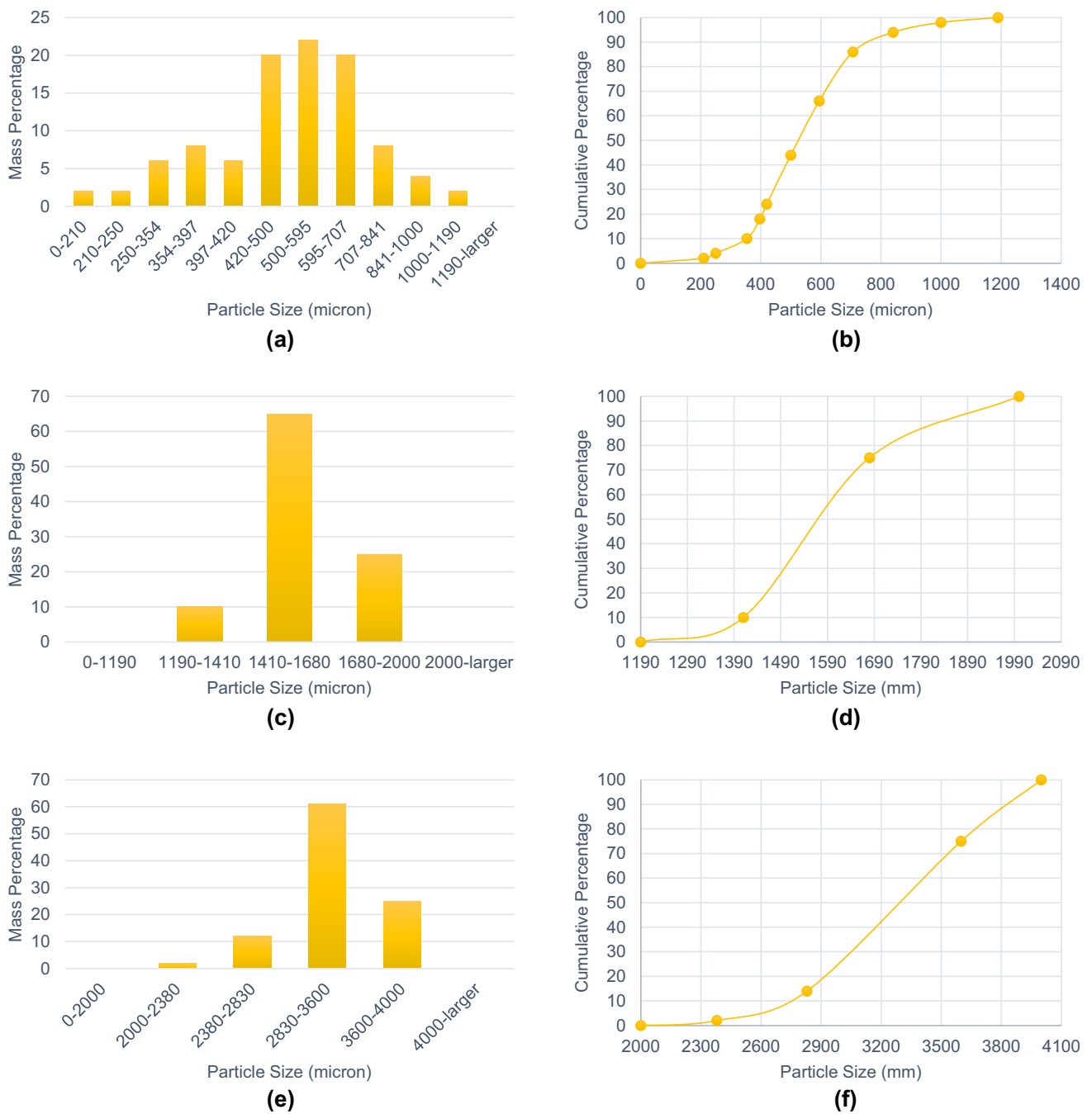


**Fig. 9** **a** Sugarcane Bagasse Fiber particle size distribution (0–1190 micron). **b** Sugarcane Bagasse Fiber cumulative particle size distribution (0–1190 micron). **c** Sugarcane Bagasse Fiber particle size distribution (1190–2000 micron). **d** Sugarcane Bagasse Fiber cumulative

particle size distribution (1190–2000 micron). **e** Sugarcane Bagasse Fiber particle size distribution (2000–4000 microns). **f** Sugarcane Bagasse Fiber cumulative particle size distribution (2000–4000 microns)

where  $W$  = Percentage by weight retained between consecutive sieves,  $X_1$  = Weight of oven-dry aggregate passing one sieve size and retained on the next smaller sieve size or pan,  $W_T$  = Total weight of the original dry sample equals the sum ( $X_1 + X_2$ ) of all the weights of aggregate retained on sieve

sizes and includes the portion that passes the smallest size sieve used.

10. Make the basic sieve analysis a 'total retained' study by weighing the material cumulatively and then placing the material retained on one sieve right on top of the

**Table 5** LPA fluid loss results in (ml) for individual LCM

Fracture width (micron)	Concentration (ppb)	1000 (C1)			
		1	2	3	4
Case# (PSD)					
<i>LCM type</i>					
Mica	25	25	5	8	11
	50	0	2	16	27
	80	43	67	88	NC
Wheat Straw	1.5	NC	NC	88	–
	2	66	53	8	–
	2.5	42	35	57	–
Oak Shell	3	7	10	21	45
	6	2	4	6	25
	10	45	57	84	NC
Sugarcane Bagasse Fiber (Canes)	3	6	12	14	43
	6	3	4	11	65
	10	29	43	66	89

**Table 6** LPA fluid loss results in (ml) for individual LCM

Fracture width (micron)	Concentration (ppb)	3000 (C2)			
		1	2	3	4
Case# (PSD)					
<i>LCM type</i>					
Mica	25	16	19	24	37
	50	15	21	33	54
	80	27	37	59	85
Wheat Straw	1.5	NC	NC	NC	–
	2	NC	NC	33	–
	2.5	NC	87	NC	–
Oak Shell	3	23	31	NC	76
	6	13	17	NC	43
	10	44	77	NC	NC
Sugarcane Bagasse Fiber (Canes)	3	20	22	23	69
	6	18	20	22	74
	10	34	43	49	86

already weighed material from the bigger sieve, which is already balanced. Take note of the difference.

- During the sieving process, take care not to lose any material. If there is a small discrepancy (less than 0.2%) between the original dry weight of the sample and the sum of the weights of the various sizes, use the original weight; if the discrepancy is large (greater than 0.2%), check the weights of the various sizes or rerun the analysis with a new sample to correct the error.

- Plot  $W$  versus particle size to get the particle size value at  $W=50\%$  ( $D_{50}$ ).

## Mud synthesis

The second stage of attempting is to make mud. We aggravate the mud subsequently identified by Tom by immersing it in bentonite and purified water. Additionally, mix it well. Our primary fixation may be 24 lb./bbl. or 24 g/350cc in a research center. To begin, add 24 g of bentonite to 350 cc of water. Furthermore, blend it for 20 min, and have LCM beneath the mud. Additionally, mix for 5 min.

## Determining the Mud's properties

During this time, we evaluate the mud's properties. In the direction of the V-G meter. A method for determining the mud-rheology Tom eventually peruses the V-G meter instrument:

- Place an as-of-late foment example in the cup, re-tilt the V-G meter's top housing, locate the container beneath the sleeve (the pins on the base of the glass fit into the gaps in the base plate), re-tilt the upper housing to its normal position.
- Switch the knurled handle back and forth between the back backings. Entries increase or ease the rotor sleeve until it is soaked in the scribed accordance's example.
- Combine those instances for approximately 5 s toward 600 RPM and select the desired rpm for those best.
- Remain seated for those dial readings with a settle (the period depends on the sample's parameters).
- Take note of the dial reading and revolutions per minute.

A simple water-base mud has been prepared. Table 1 represents the test mud formulation. Table 2 illustrates the test mud rheology. As shown in Fig. 3, the mud behavior follows the Herschel-Bulkley model. The rheological behavior of mud in the Herschel-Bulkley model is as follows:

$$\tau = \tau_y + k \left( -\frac{dv}{dz} \right)^m \quad (2)$$

where  $\tau_y$  is yield stress,  $k$  and  $m$  are model constants.

## Particle bridging tests

The particle bridging experiments were conducted on water-base mud with different LCM types. The tests have been carried out using two cell types, several LCMs with different concentrations, and PSDs. Figure 4 shows two cells with varying widths of fracture that simulate sealable fractures with tip sizes of 1000 microns and 3000 microns (Table 3).

**Table 7** Summary of HPA testing results for Mica

Test no.	LCM type	Cell	Concentration (ppb)	Case number	LPA fluid loss (ml)	Maximum sealing pressure (psi)	Total fluid loss (ml)	Average fluid loss (ml/cycle)
1	Mica	C1	25	1	2	1905	7	2.33
2			25	2	5	1831	17	5.67
3			25	3	8	1855	31	7.75
4			25	4	11	1197	45	15
5			50	1	0	2123	6	1
6			50	2	2	1987	7	1.75
7			50	3	16	1060	40	20
8			50	4	27	599	71	35.5
9		C2	25	1	16	1841	85	21.25
10			25	2	19	1727	86	28.67
11			25	3	24	955	95	31.67
12			25	4	37	700	98	98
13			50	1	15	1969	79	15.8
14			50	2	21	1608	89	22.25
15			50	3	33	684	98	24.5
16			50	4	54	449	NC	NC

**Table 8** Summary of HPA testing results for Wheat Straw

Test no.	LCM type	Cell	Concentration (ppb)	Case number	LPA fluid loss (ml)	Maximum sealing pressure (psi)	Total fluid loss (ml)	Average fluid loss (ml/cycle)
1	Wheat Straw	C1	2	1	66	619	98	19.60
2			2	2	53	599	57	57
3			2	3	8	1108	37	9.25
4			2.5	1	42	1002	93	31
5			2.5	2	35	524	65	32.50
6			2.5	3	57	234	NC	NC
7		C2	2	1	NC	355	NC	NC
8			2	2	NC	427	NC	NC
9			2	3	33	619	95	31.67
10			2.5	1	NC	85	NC	NC
11			2.5	2	87	295	NC	NC
12			2.5	3	NC	140	NC	NC

Several different formulations for each LCM type and total concentration were tested to study the particle size distribution (PSD) effect on particle bridging. Table 4 shows the weight percentage of each LCM in total concentration when it is used individually to develop any given case.

#### Apparatus for low-pressure testing (LPA)

The test can be conducted by filling the transfer vessel half-way with the 500 cc fluid containing LCMs and then gradually applying 100 psi through the air compressor to push

the fluid through the cell until no more fluid comes out. The critical parameter here is the volume of fluid lost in 30 min. This qualitative metric indicates if the Concentration, PSD, can seal a particular fracture width. The LPA is a simple, rapid indicator of the LCM's performance, and its results can guide future investigations at greater pressures using the high-pressure apparatus. The low-pressure LCM testing apparatus is shown in Fig. 5.

**Table 9** Summary of HPA testing results for Oak Shell

Test no.	LCM type	Cell	Concentration (ppb)	Case number	LPA fluid loss (ml)	Maximum sealing pressure (psi)	Total fluid loss (ml)	Average fluid loss (ml/cycle)	
1	Oak Shell	C1	3	1	7	1195	36	7.20	
2			3	2	10	1000	34	11.33	
3			3	3	21	502	87	14.50	
4			3	4	45	340	97	24.25	
5			6	1	2	2291	8	2	
6			6	2	4	1731	31	31	
7			6	3	6	1269	19	4.75	
8			6	4	25	1014	81	16.20	
9		C2		3	1	23	973	92	30.67
10				3	2	31	677	98	32.67
11				3	3	NC	161	NC	NC
12				3	4	76	304	NC	NC
13				6	1	13	2203	67	16.75
14				6	2	17	1649	94	94
15				6	3	NC	241	NC	NC
16				6	4	43	436	NC	NC

**Table 10** Summary of HPA testing results for Sugarcane Bagasse Fiber (Canes)

Test no.	LCM type	Cell	Concentration (ppb)	Case number	LPA fluid loss (ml)	Maximum sealing pressure (psi)	Total fluid loss (ml)	Average fluid loss (ml/cycle)	
1	Sugarcane Bagasse Fiber (Canes)	C1	3	1	6	1569	31	5.17	
2			3	2	12	1228	81	10.12	
3			3	3	14	1272	80	13.33	
4			3	4	43	1087	NC	NC	
5			6	1	3	1893	13	2.6	
6			6	2	4	1740	27	4.50	
7			6	3	11	1656	33	11	
8			6	4	65	1170	NC	NC	
9		C2		3	1	20	1382	89	17.8
10				3	2	22	1117	97	24.25
11				3	3	23	1081	98	19.60
12				3	4	69	916	NC	NC
13				6	1	18	1553	85	14.17
14				6	2	20	1360	91	18.2
15				6	3	22	1219	98	16.33
16				6	4	74	1109	NC	NC

### Testing of a high-pressure apparatus (HPA)

The high-pressure apparatus was designed to withstand up to 10,000 psi pressure. The transfer vessel is filled with 500 cc of pill (mud-containing LCM). The test is conducted by introducing LCM-containing fluids at a 30 ml/min flow rate until a rapid increase in the injection pressure is detected. A

large pressure decrease is seen due to the seal being broken and the development of a pressure cycle. A cycle is defined as any pressure drop equal to or greater than 100 psi. The high-pressure LCM testing apparatus is shown in Fig. 5.

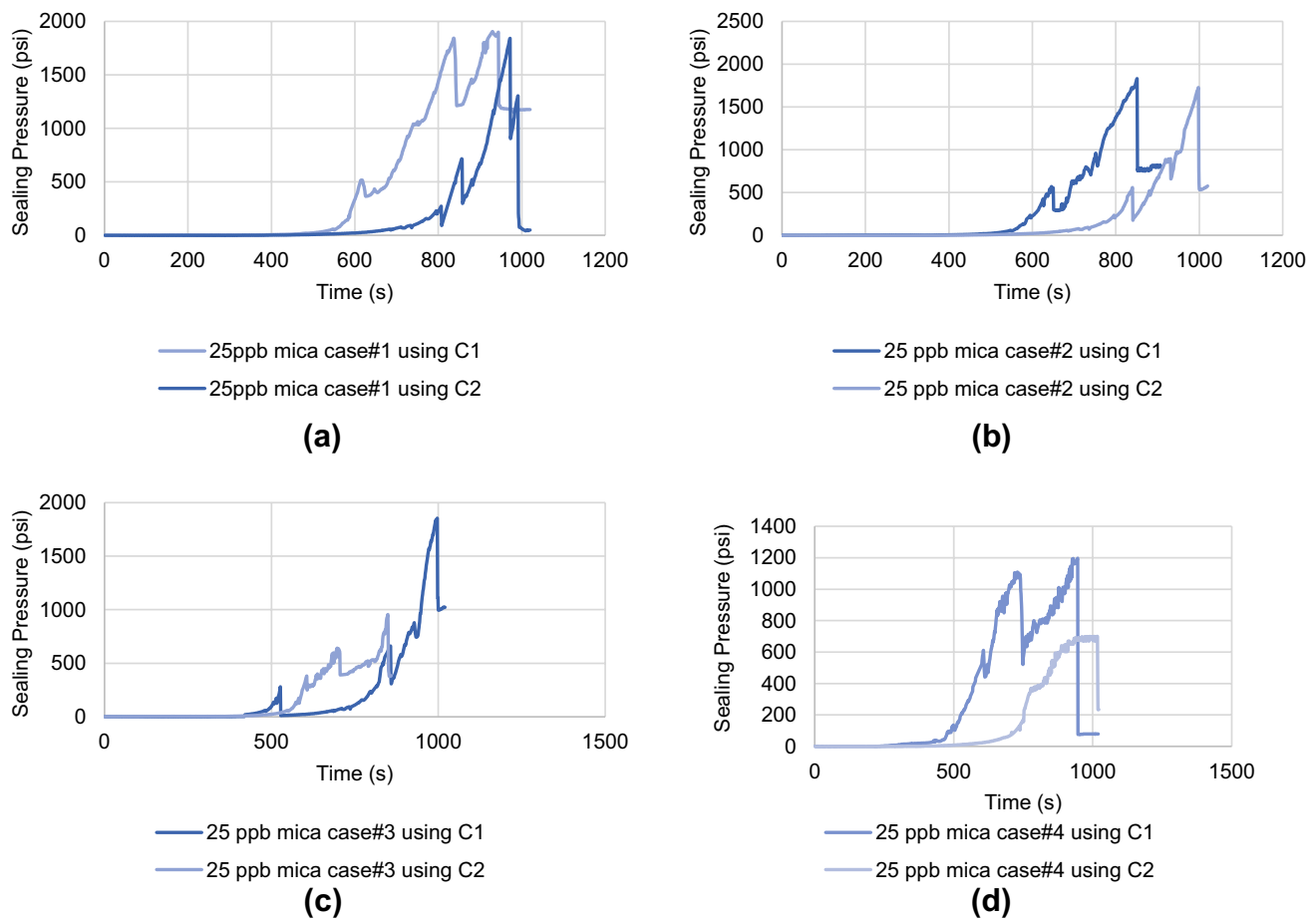


**Fig. 10** HPA Pressure versus Time plot for 25 ppb Mica showing maximum sealing pressure at different fracture widths, **a** case#1, **b** case#2, **c** case#3, **d** case#4

## Results and discussion

### Particle size distribution (PSD) measurements

The particle size distribution for each LCM was conducted. PSD for ranges 0–1.19 mm, 1.19–1.68 mm, 1.68–2 mm, and 2–4 mm, and cumulative distribution and D50 for mentioned ranges were done. PSD and cumulative PSD for each blend is shown in Figs. 6, 7, 8 and 9.

### Particle bridging tests

#### Low-pressure apparatus test (LPA)

The LPA was a simple, fast, reliable test to ensure that the selected LCM type and concentration seal a specific fracture width. One hundred-two instances were tested to optimize the LCM combinations and concentrations. The results are listed in Tables 5 and 6 for individual LCM. If the fluid loss value goes over 100 ml, it is non-controlled (NC). Four different formulations for each LCM type were tested

individually at several concentrations. As we see in Tables 5 and 6, increasing the concentration of LCM will decrease the volume of fluid loss. However, a critical maximum concentration threshold existed that exceeding this quantity would result in an abrupt increase in fluid loss.

#### High-pressure apparatus test (HPA)

Seventy-two tests were conducted to evaluate the integrity of the seal formed using the HPA. The results are summarized in Tables 7, 8, 9 and 10. The fluid loss values from the screening tests included in the table are comparable with the fluid loss per cycle values. The applied pressure to the seal, formed in fracture, is recorded as time by a computer. According to the recorded pressure curve, the maximum sealing pressure and the number of times the seal is broken (number of cycles) can be determined. The following curves show the relationship between pressure and time for different cases, concentrations, fracture width, and LCM types, as shown in Tables 7, 8, 9 and 10. As fluid loss value decreases, maximum sealing pressure increases. Also, it

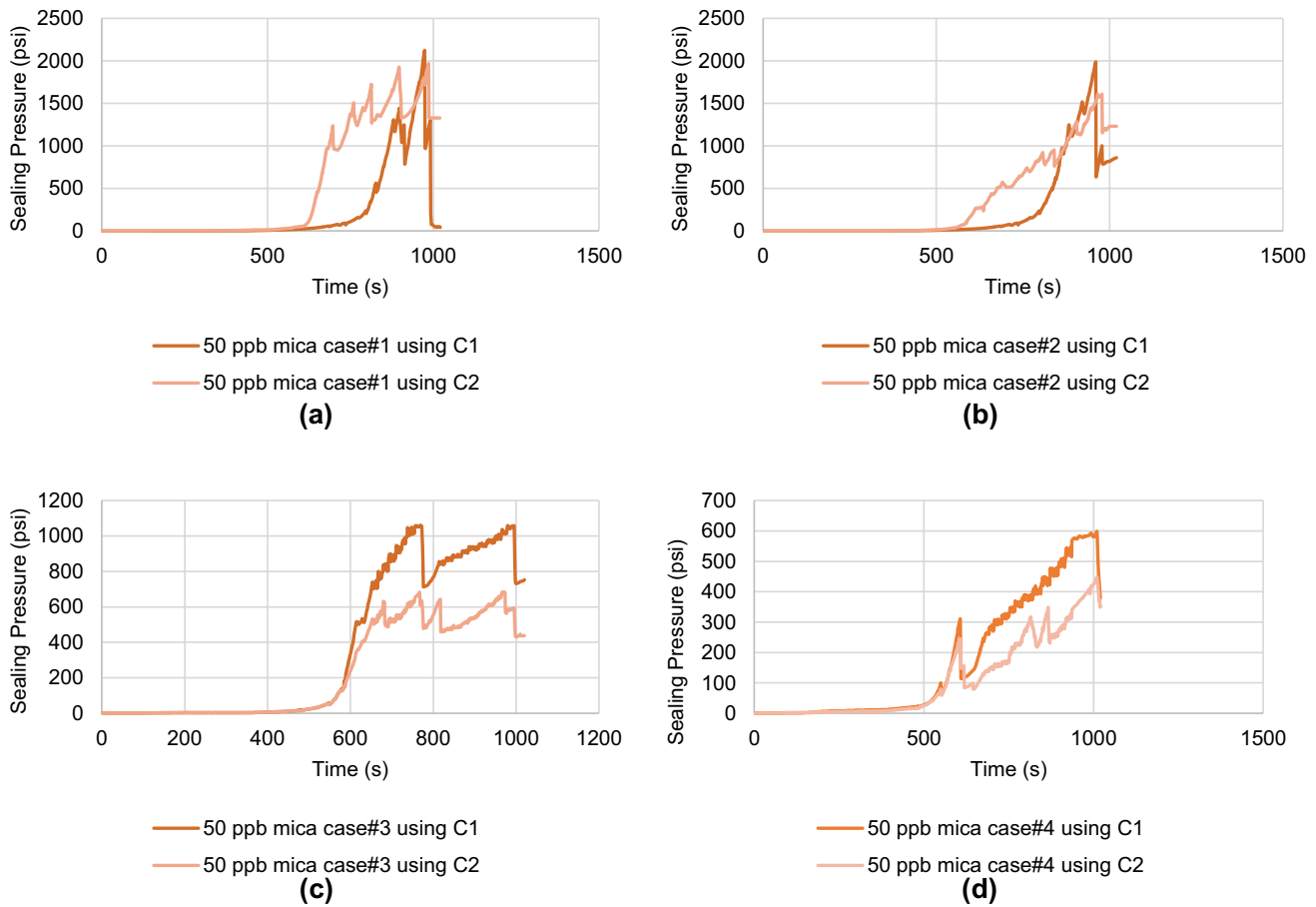


**Fig. 11** HPA Pressure versus Time plot for 50 ppb Mica showing maximum sealing pressure at different fracture widths, **a** case#1, **b** case#2, **c** case#3, **d** case#4

is demonstrated that Oak Shells and Mica blends have the minimum and maximum value in fluid loss and maximum sealing pressure, respectively.

**Test with Mica LCM blend Fracture width effect** Figure 10a–d shows the maximum sealing pressure using a 25 ppb Mica blend when tested at different fracture widths and four different PSDs; case#1 (a), case#2 (b), case#3 (c), and case#4 (d). A 3.4%, 5.7%, 48.5%, and 64.6% decrease (1905 to 1841, 1831 to 1727, 1855 to 955, and 1977 to 700 psi) in the sealing pressure for 25 ppb Mica blend was observed when the fracture width was increased from 1 to 3 mm for case#1 (a), case#2 (b), case#3 (c) and case#4 (d), respectively. Figure 11a–d shows the maximum sealing pressure using a 50 ppb Mica blend when tested at different fracture widths and four different PSDs; case#1 (a), case#2 (b), case#3 (c), and case#4 (d). A 2.4%, 19.1%, 35.5%, and 16.5% decrease (2123 to 2071, 1987 to 1608, 1060 to 684, and 599 to 449 psi) in the sealing pressure for 50 ppb Mica blend was observed when the fracture width was increased from 1 to 3 mm for case#1 (a), case#2 (b), case#3

(c) and case#4 (d), respectively. As illustrated in Figs. 10a, b, 11a, and b, it is found that with increasing fracture width from 1000 microns to 3000 microns, there is no considerable reduction in maximum sealing pressure, *i.e.*, in case of appropriate selection of PSD, any change in fracture width does not affect Mica blend functionality.

**Concentration effect** Figure 12a–d show the maximum sealing pressure for the Mica blend using C1 when tested at different concentrations and four different PSD; case#1 (a), case#2 (b), case#3 (c), and case#4 (d). An 11.4% and 8.5% increase (1905 to 2123, 1831 to 1987 psi) and a 42.9%, 49.9% decrease (1855 to 1060 and 1197 to 599 psi) in the sealing pressure for Mica blend was observed when concentration was increased by 100% from 25 to 50 ppb for case#1 (a), case#2 (b), case#3 (c) and case#4 (d), respectively. Figure 13a–d shows the maximum sealing pressure for the Mica blend using C2 when tested at different concentrations and four different PSDs; case#1 (a), case#2 (b), case#3 (c), and case#4 (d). A 6.9% increase (1841 to 1969 psi) and a 6.9%, 28.4%, and 35.9% decrease (1727 to 1608, 955 to 684, and 700 to 449 psi) in the sealing pressure for Mica blend



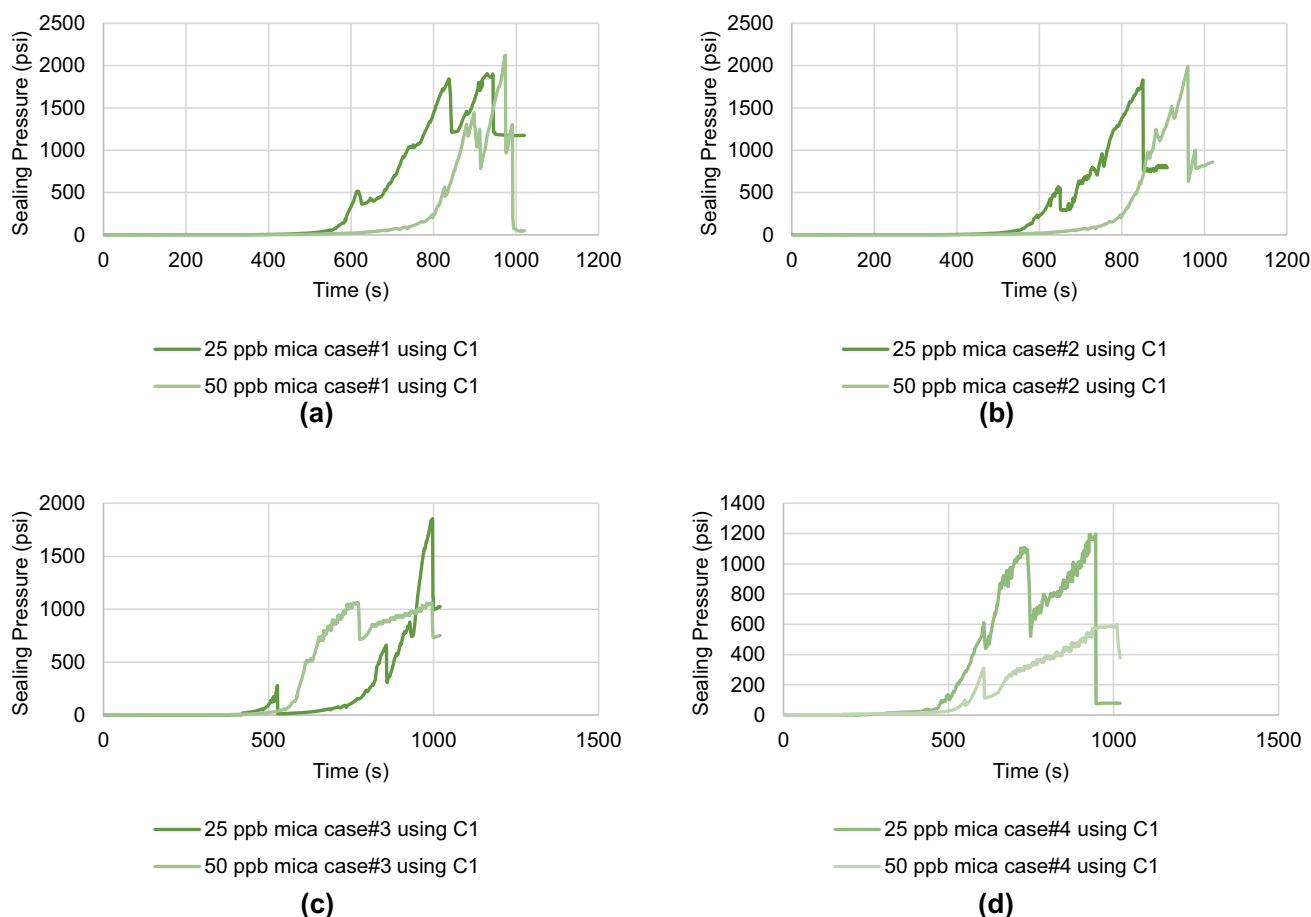


**Fig. 12** HPA Pressure versus Time plot for Mica showing maximum sealing pressure at different concentration, **a** case#1, **b** case#2, **c** case#3, **d** case#4

was observed when concentration was increased by 100% from 25 to 50 ppb for case#1 (a), case#2 (b), case#3 (c) and case#4 (d), respectively. As expected, maximum sealing pressure increases; however, it has a reverse effect (Figs. 12c, d, 13c, d). The reasons for this are that the amount of coarse particle concentration is excessively increased, which does not allow penetration of particles into the fracture, or some of these particles are stuck in the opening in the end part of the transfer vessel and thus reducing the amount of output LCM; therefore, a proper seal is not formed.

**PSD effect** Figure 14a shows the maximum sealing pressure using 25 ppb Mica blend and C1 when tested in different cases (case#1, case#2, case#3, and #4). When C1 was used, the sealing pressure using case#2, case#3, and case#4 dropped from 1905 to 1831 psi (3.8%), 1905 to 1855 psi (2.6%), and 1905 to 1197 psi (37.2%), respectively, relative to case#1. Figure 14b shows the maximum sealing pressure using 25 ppb Mica blend and C2 when tested in different

cases (case#1, case#2, case#3, and case#4). When C2 was used, the sealing pressure using case#2, case#3, and case#4 dropped from 1841 to 1727 psi (6.2%), 1841 to 955 psi (48.1%), and 1841 to 700 psi (62%), respectively, relative to case#1. Figure 14c shows the maximum sealing pressure using 50 ppb Mica blend and C1 when tested in different cases (case#1, case#2, case#3, and case#4). When C1 was used, the sealing pressure using case#2, case#3, and case#4 dropped from 2123 to 1987 psi (6.4%) and 2123 to 1060 psi (50.1%), and 2123 to 599 psi (71.8%), respectively, relative to case#1. Figure 14d shows the maximum sealing pressure using 50 ppb Mica blend and C2 when tested in different cases (case#1, case#2, case#3, and case#4). When C2 was used, the sealing pressure using case#2, case#3, and case#4 dropped from 1969 to 1608 (18.3%), 1969 to 684 psi (65.3%), and 1969 to 449 psi (77.2%), respectively, relative to case#1. As seen in Fig. 14a–d, using vastly distributed

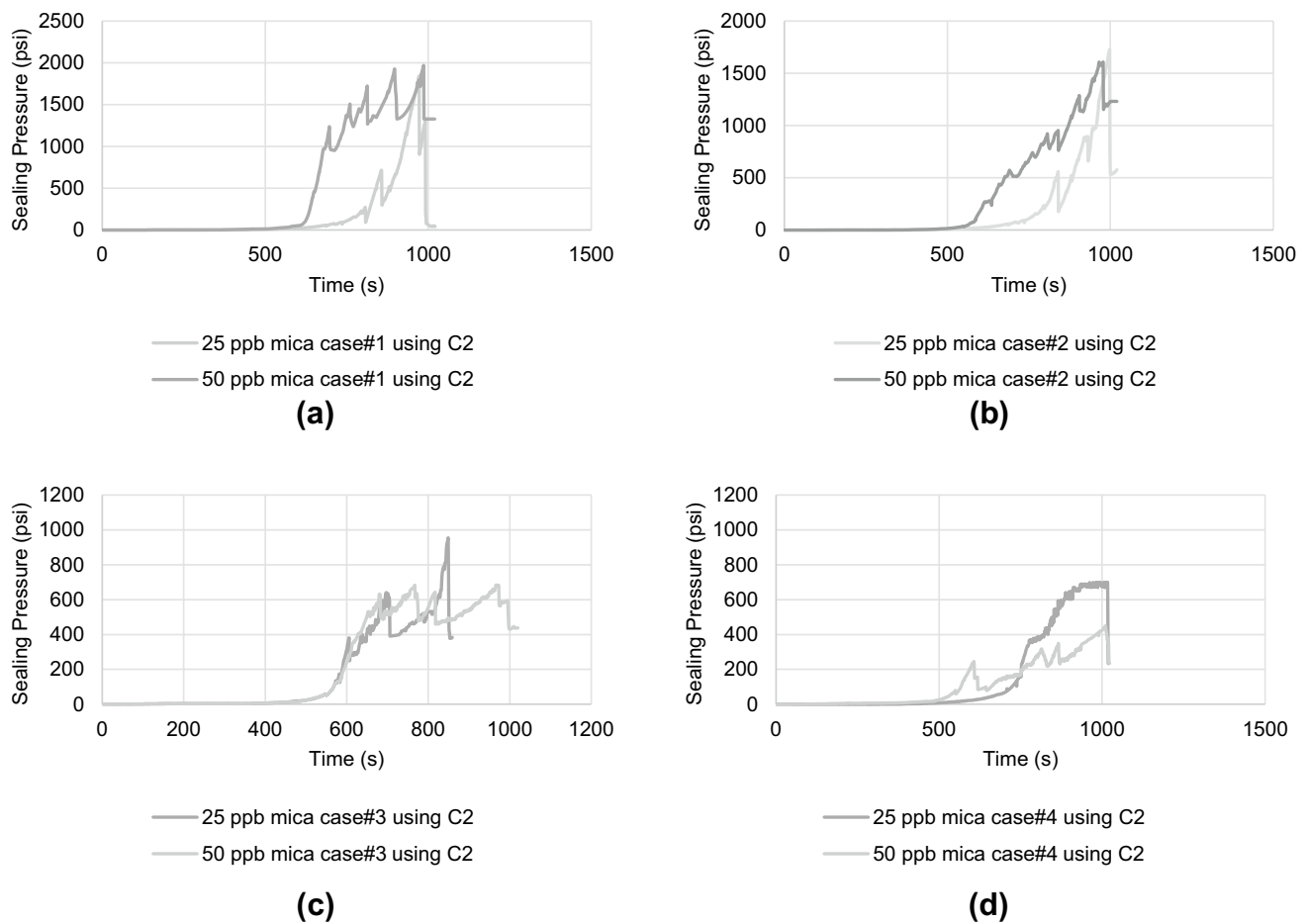


**Fig. 13** HPA Pressure versus Time plot for Mica showing maximum sealing pressure at different concentrations, **a** case#1, **b** case#2, **c** case#3, **d** case#4

particles, such as cases #1 and #2, would give more relevant results.

**Test with Canes LCM blend** *Fracture width effect* Figure 15a–d shows the maximum sealing pressure using three ppb Canes blends when tested at different fracture widths and four different PSDs; case#1 (a), case#2 (b), case#3 (c), and case#4 (d). A 9%, 9%, 15%, and 15.7% decrease (1569 to 1382, 1228 to 1117, 1272 to 1081 and 1087 to 916 psi) in the sealing pressure for 3 ppb Canes blend was observed when the fracture width was increased from 1 to 3 mm for case#1 (a), case#2 (b), case#3 (c) and case#4 (d), respectively. Figure 16a–d shows the maximum sealing pressure using six ppb Canes blends when tested at different fracture widths and four different PSDs; case#1 (a), case#2 (b), case#3 (c), and case#4 (d). An 18%,

21.8%, 26.4%, and 5.2% decrease (1893 to 1553, 1740 to 1360, 1656 to 1219, and 1170 to 1109 psi) in the sealing pressure for 3 ppb Canes blend was observed when the fracture width was increased from 1 to 3 mm for case#1 (a), case#2 (b), case#3 (c) and case#4 (d), respectively. As is obvious in all the graphs, maximum sealing pressure decreases with increasing fracture width.

*Concentration effect* Figure 17a–d shows the maximum sealing pressure for the Canes blend using C1 when tested at different concentrations and four different PSDs; case#1 (a), case#2 (b), case#3 (c), and case#4 (d). A 20.6%, 41.7%, 30.2%, and 7.6% increase (1569 to 1893, 1228 to 1740, 1272 to 1656, and 1087 to 1170 psi) in the sealing pressure for Mica blend was observed when concentration was increased by 100% from 3 to 6 ppb for case#1 (a), case#2 (b), case#3 (c), and case#4 (d), respectively. Figure 18a–d shows the

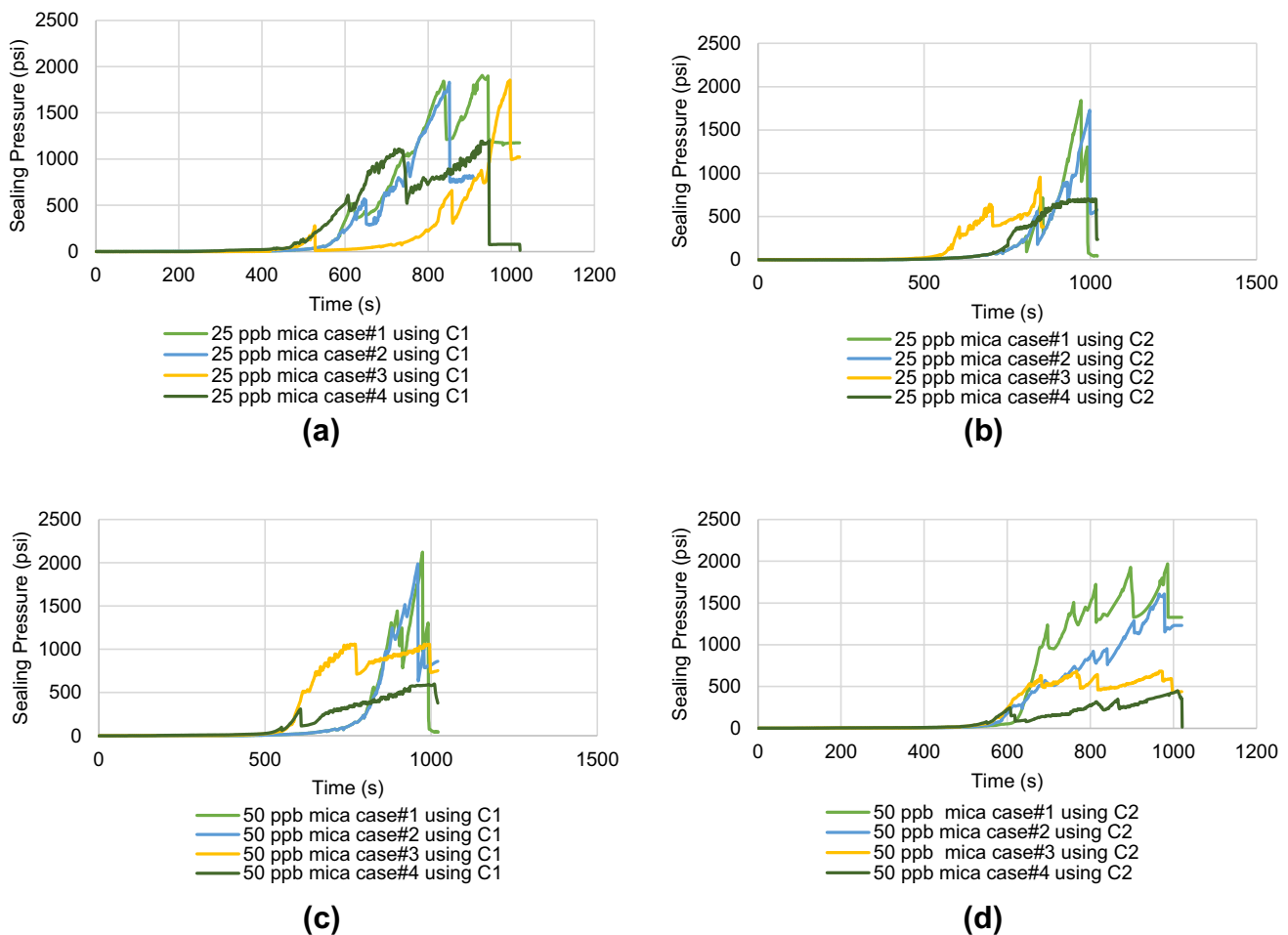


**Fig. 14** HPA Pressure versus Time plot for 25 & 50 ppb Mica showing maximum sealing pressure at different cases using C1 and C2

maximum sealing pressure for the Canes blend using C2 when tested at different concentrations and four different PSDs; case#1 (a), case#2 (b), case#3 (c), and case#4 (d). A 12.4%, 21.7%, 12.8%, and 21.1% increase (1382 to 1553, 1117 to 1360, 1081 to 1219, and 916 to 1109 psi) in the sealing pressure for Canes blend was observed when concentration was increased by 100% from 3 to 6 ppb for case#1 (a), case#2 (b), case#3 (c) and case#4 (d), respectively. As is obvious in all the graphs, maximum sealing pressure increases with increasing concentration.

**PSD effect** Figure 19a shows the maximum sealing pressure using three ppb Canes blend and C1 when tested in different cases (case#1, case#2, case#3, and case#4). When C1 was used, the sealing pressure using case#2, case#3, and case#4 dropped from 1569 to 1228 psi (21.7%), 1719 to 1272 psi (18.9%), and 1569 to 1087 psi (30.7%), respectively, relative to case#1. Figure 19b shows the maximum sealing

pressure using three ppb Canes blend and C2 when tested in different cases (case#1, case#2, case#3, and #4). When C2 was used, the sealing pressure using case#2, case#3, and case#4 dropped from 1382 to 1117 psi (19.2%), 1382 to 1081 psi (21.8%), and 1382 to 916 psi (33.7%), respectively, relative to case#1. Figure 19c shows the maximum sealing pressure using six ppb Canes blend and C1 when tested in different cases (case#1, case#2, case#3, and case#4). When C1 was used, the sealing pressure using case#2, case#3, and case#4 dropped from 1893 to 1740 psi (8.1%), 1893 to 1656 psi (12.5%), and 1893 to 1170 psi (38.2%), respectively, relative to case#1. Figure 19d shows the maximum sealing pressure using six ppb Canes blend and C2 when tested in different cases (case#1, case#2, case#3, and #4). When C2 was used, the sealing pressure using case#2, case#3, and case#4 dropped from 1553 to 1360 (12.4%), 1553 to 1219 psi (21.5%), and 1553 to 1109 psi (28.6%), respectively,

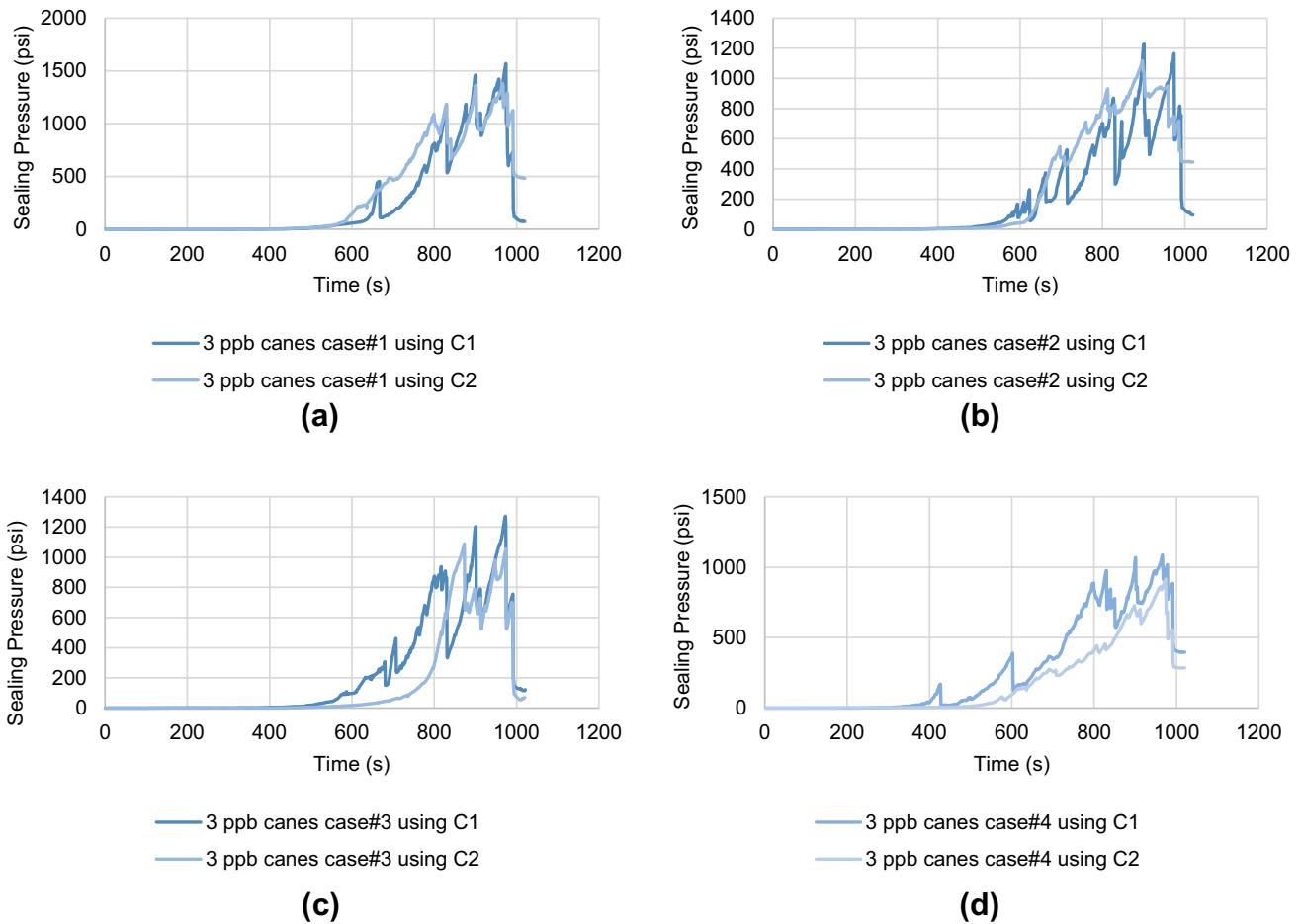


**Fig. 15** HPA Pressure versus Time plot for 3 ppb Canes showing maximum sealing pressure at different fracture widths, **a** case#1, **b** case#2, **c** case#3, **d** case#4

relative to case#1. As seen in Fig. 19a–d, using vastly distributed particles, such as cases #1 and case#2, would give better results.

#### Test with Wheat Straw LCM blend Fracture width effect

Figure 20a–c shows the maximum sealing pressure using a 2 ppb Wheat Straw blend when tested at different fracture widths and four different PSDs; case#1 (a), case#2 (b), and case#3 (c). A 31%, 29%, and 44.1% decrease (619 to 355, 599 to 427, and 1108 to 619 psi) in the sealing pressure for two ppb Wheat Straw blends was observed when the fracture width was increased from 1 to 3 mm for case#1 (a), case#2 (b) and case#3 (c), respectively. Figure 20d–f shows the maximum sealing pressure using a 2.5 ppb Wheat Straw blend when tested at different fracture widths and four different PSDs; case#1 (d), case#2 (e), and case#3 (f). A 91%, 44%, and 40% decrease (1002 to 85, 524 to 295, and

234 to 140 psi) in the sealing pressure for two ppb Wheat Straw blends was observed when the fracture width was increased from 1 to 3 mm for case#1 (d), case#2 (e), and case#3 (f), respectively. As shown in all the graphs, maximum sealing pressure decreases with increasing fracture width.

**Concentration effect** Figure 21a–c shows the maximum sealing pressure for the Wheat Straw blend using C1 when tested at different concentration and four different PSD; case#1 (a), case#2 (b), and case#3 (c). A 62% increase (619 to 1002 psi) and a 12% and 79% decrease (599 to 524 and 1108 to 234 psi) in the sealing pressure for the Wheat Straw blend were observed when concentration was increased by 25% from 2 to 2.5 ppb for case#1 (a), case#2 (b) and case#3 (c), respectively. Figure 21d–f shows the maximum sealing pressure for the Wheat Straw blend using

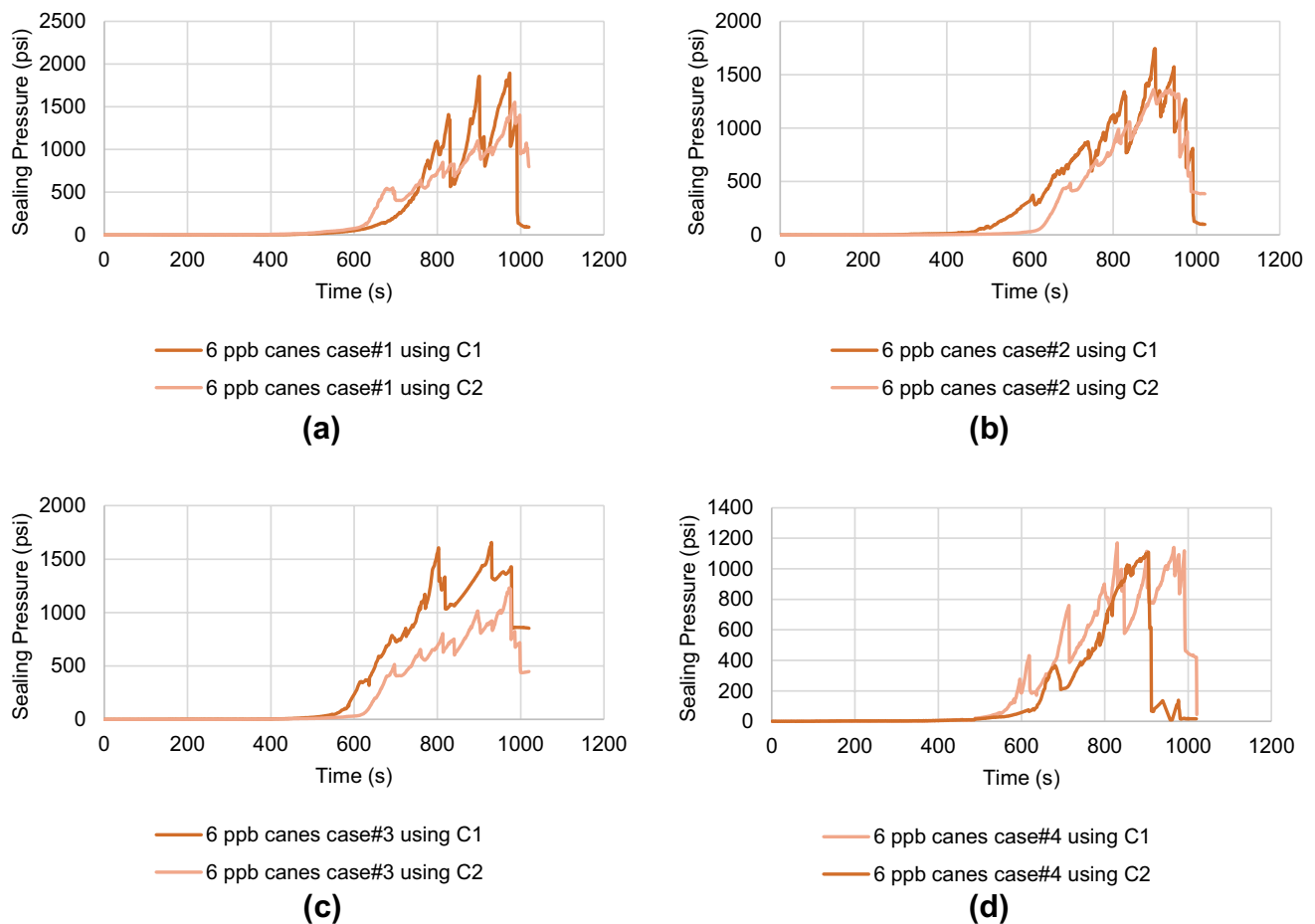


**Fig. 16** HPA Pressure versus Time plot for 6 ppb Canes showing maximum sealing pressure at different fracture widths, **a** case#1, **b** case#2, **c** case#3, **d** case#4

C2 when tested at different concentrations and four different PSDs; case#1 (d), case#2 (e), and case#3 (f). An 80%, 30.9%, and 77.4% decrease (355 to 85, 427 to 295, and 619 to 140 psi) in the sealing pressure for the Wheat Straw blend was observed when concentration was increased by 25% from 2 to 2.5 ppb for case#1 (d), case#2 (e), and case#3 (f), respectively. As seen in Fig. 21b–f, increasing the concentration of the Wheat Straw blend from 2 to 2.5 ppb increases the maximum sealing pressure. The reasons for this are that the amount of coarse particle concentration is excessively increased, which does not allow penetration of particles into the fracture, or some of these particles are stuck in the opening in the end part of the transfer vessel and thus reducing the amount of output LCM; therefore, a proper seal is not formed. So the concentration of 2 ppb is the optimized value for the Wheat Straw blend.

*PSD effect* Figure 22 shows the maximum sealing pressure using two ppb Wheat Straw blends and C1 when tested in different cases (case#1, case#2, case#3, and case#4). When C1 was used, the sealing pressure using case#2 and case#1 dropped from 619 to 599 psi (3.2%), and using case#3 increased from 619 to 1108 psi (79%), respectively. Figure 22b shows the maximum sealing pressure using two ppb Wheat Straw blends and C2 when tested in different cases (case#1, case#2, case#3, and case#4). When C2 was used, the sealing pressure using both case#2 and case#3 increased from 355 to 427 psi (20.3%) and 355 to 619 psi (74.4%), respectively, relative to case#1. Figure 22c shows the maximum sealing pressure using 2.5 ppb Wheat Straw blend and C1 when tested in different cases (case#1, case#2, case#3, and case#4). When C1 was used, the sealing pressure using both case#2 and case#3 dropped from 1002 to 534 psi (47.7%) and 1002 to 234 psi (76.6%), respectively,

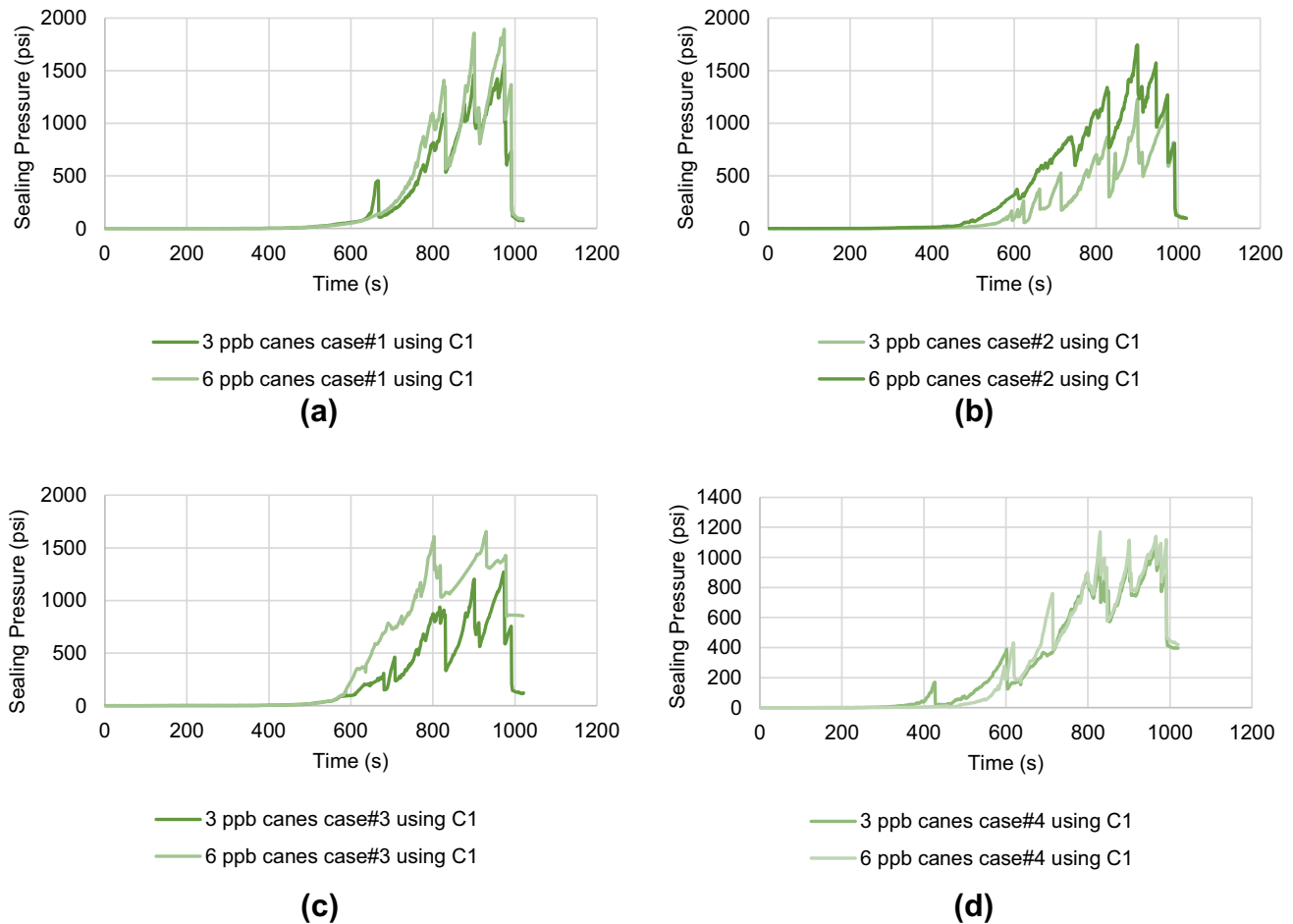


**Fig. 17** HPA Pressure versus Time plot for Canes showing maximum sealing pressure at different concentrations, **a** case#1, **b** case#2, **c** case#3, **d** case#4

relative to case#1. Figure 22d shows the maximum sealing pressure using 2.5 ppb Wheat Straw blend and C2 when tested in different cases (case#1, case#2, case#3, and case#4). When C2 was used, the sealing pressure using both case#2 and case#3 increased from 85 to 295 psi (247%), and 85 to 140 psi (64.7%), respectively, relative to case#1. As shown in Fig. 22a, b, using vastly distributed particles such as case#3 would give more relevant results. But, the maximum sealing pressure of case#3 shows a significant decrease in Fig. 22c, d. This happens because large particles' concentration is greater than the critical concentration.

**Test with Oak Shell LCM blend** *Fracture width effect* Figure 23a–d shows the maximum sealing pressure using three ppb Oak Shell blends when tested at different fracture widths and four different PSDs; case#1 (a), case#2 (b), case#3 (c), and case#4 (d). An 18.6%, 32.3%, 67.9%,

and 10.6% decrease (1195 to 973, 1000 to 677, 502 to 161, and 340 to 304 psi) in the sealing pressure for three ppb Oak Shell blend was observed when the fracture width was increased from 1 to 3 mm for case#1 (a), case#2 (b), case#3 (c) and case#4 (d), respectively. Figure 24a–d shows the maximum sealing pressure using a 6 ppb Oak Shell blend when tested at different fracture widths and four different PSDs; case#1 (a), case#2 (b), case#3 (c), and case#4 (d). 3.28%, 4.7%, 81%, and 57% decrease (2291 to 2203, 1731 to 1649, 1269 to 241, and 1014 to 436 psi) in the sealing pressure for six ppb Oak Shell blend was observed when the fracture width was increased from 1 to 3 mm for case#1 (a), case#2 (b), case#3 (c), and case#4 (d), respectively. As expected in all the graphs, maximum sealing pressure decreases with increasing fracture width.

*Concentration effect* Figure 25a–d shows the maximum sealing pressure for the Oak Shell blend using C1 when



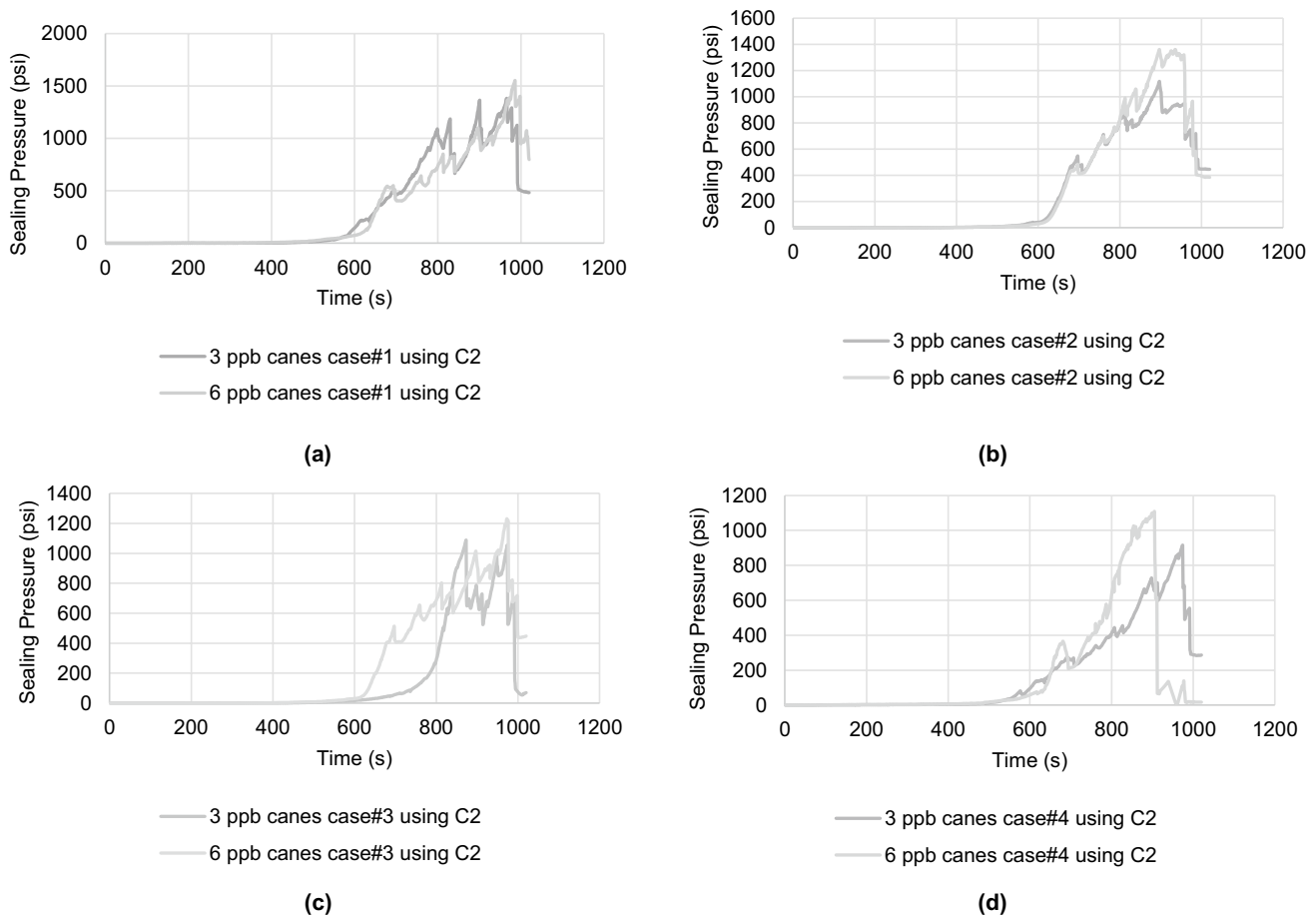


**Fig. 18** HPA Pressure versus Time plot for Canes showing maximum sealing pressure at different concentrations, **a** case#1, **b** case#2, **c** case#3, **d** case#4

tested at different concentration and four different PSDs; case#1 (a), case#2 (b), case#3 (c), and case#4 (d). A 91.7%, 73.1%, 152.8%, and 198.2% increase (1195 to 2291, 1000 to 1731, 502 to 1269, and 340 to 1014 psi) in the sealing pressure for Oak Shell blend was observed when concentration was increased by 100% from 3 to 6 ppb for case#1 (a), case#2 (b), case#3 (c), and case#4 (d), respectively. Figure 26a–d shows the maximum sealing pressure for the Oak Shell blend using C2 when tested at different concentrations and four different PSDs; case#1 (a), case#2 (b), case#3 (c), and case#4 (d). A 126.4%, 143.6%, 49.7%, and 43.4% increase (973 to 2203, 677 to 1649, 161 to 241, and 304 to 436 psi) in the sealing pressure for the Oak Shell blend was observed when concentration was increased by 100% from 3 to 6 ppb for case#1 (a), case#2 (b), case#3 (c), and case#4 (d), respectively. As shown in all the graphs, by doubling

the concentration of the Oak Shell blend from 3 to 6 ppb, the maximum sealing pressure value increases excessively.

*PSD effect* Figure 27 shows the maximum sealing pressure using three ppb Oak Shell blends and C1 when tested in different cases (case#1, case#2, case#3, and case#4). When C1 was used, the sealing pressure using case#2, case#3, and case#4 dropped from 1195 to 1000 psi (16.3%), 1195 to 502 psi (58%), and 1195 to 340 psi (71.5%), respectively, relative to case#1. Figure 27b shows the maximum sealing pressure using three ppb Oak Shell blends and C2 when tested in different cases (case#1, case#2, case#3, and case#4). When C2 was used, the sealing pressure using case#2, case#3, and case#4 dropped from 973 to 677 psi (30.4%), 973 to 161 psi (83.4%), and 973 to 304 psi (68.6%), respectively, relative to case#1. Figure 27c shows the maximum sealing pressure using a six ppb Oak Shell blend and C1 when tested in different cases (case#1, case#2, case#3, and case#4). When C1

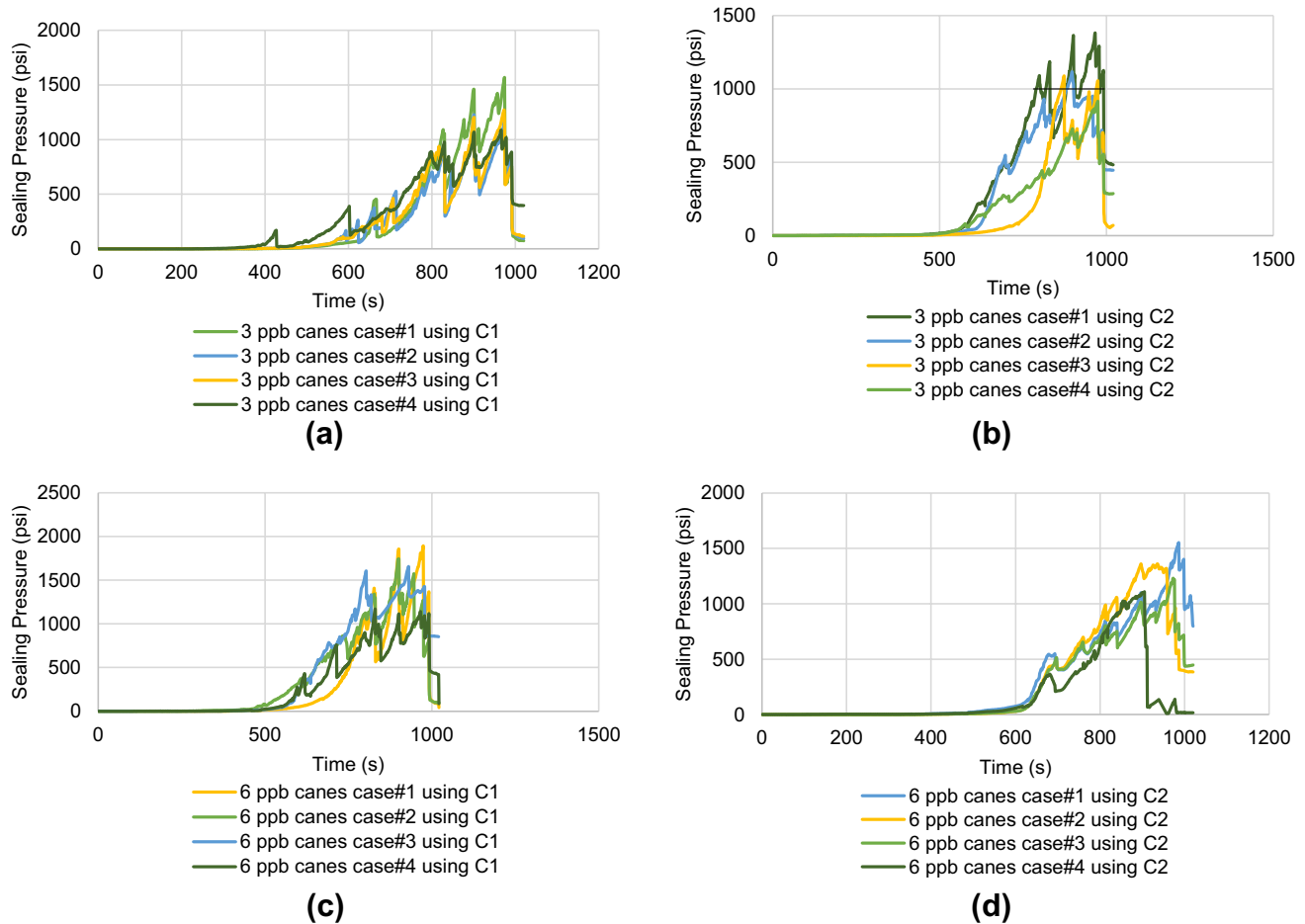


**Fig. 19** HPA Pressure versus Time plot for 3 & 6 ppb Canes showing maximum sealing pressure at different cases using C1 and C2

was used, the sealing pressure using case#2, case#3, and case#4 dropped from 2291 to 1731 psi (24.4%), 2291 to 1269 psi (44.6%), and 2291 to 1014 psi (55.7%), respectively. Figure 27d shows the maximum sealing pressure using six ppb Oak Shell blend and C2 when tested in different cases (case#1, case#2, case#3, and case#4). When C2 was used, the sealing pressure using case#2, case#3, and case#4 dropped from 2203 to 1649 (25.1%), 2203 to 241 psi (89%), and 2203 to 436 psi (80.2%), respectively, relative to case#1. As shown in Fig. 27a–d, using vastly distributed particles like case#3 would give more relevant results.

**Comparisons of tests with Mica, Wheat Straw, Canes, and Oak Shell experimental results** The best LCM type test selects the highest maximum pressure and lowest fluid loss in this section. And compare them together. Figure 28a shows the maximum sealing pressure using Mica, Canes, Oak Shell, and Wheat Straw blend, and C1 when tested

at the best particle size and concentration. When C1 was used, the sealing pressure using the Canes and Wheat Straw blend dropped from 2123 to 1893 psi (10.8%), and 2123 to 1108 (47.8%), respectively, relative to Mica blend, and using the Oak Shell blend increased from 2123 to 2291 psi (7.9%). Figure 28b shows the maximum sealing pressure using Mica, Canes, Oak Shell, and Wheat Straw blend, and C2 when tested at the best PSD and concentration. When C2 was used, the sealing pressure using the Canes and Wheat Straw blend dropped from 1969 to 1553 psi (21.1%), 1969 to 619 (68.5%), respectively, relative to Mica blend, and using the Oak Shell blend increased from 1969 to 2203 psi (11.9%). As it is shown in Fig. 28a and b, Oak Shells, Mica, Canes, and Wheat Straw blends have the best performance, respectively. After each test, the fracture inside the cell was observed. It could be concluded that increasing irregularity in particular geometry, such as the Oak Shell blend has sealed the fracture more appropriately than regu-

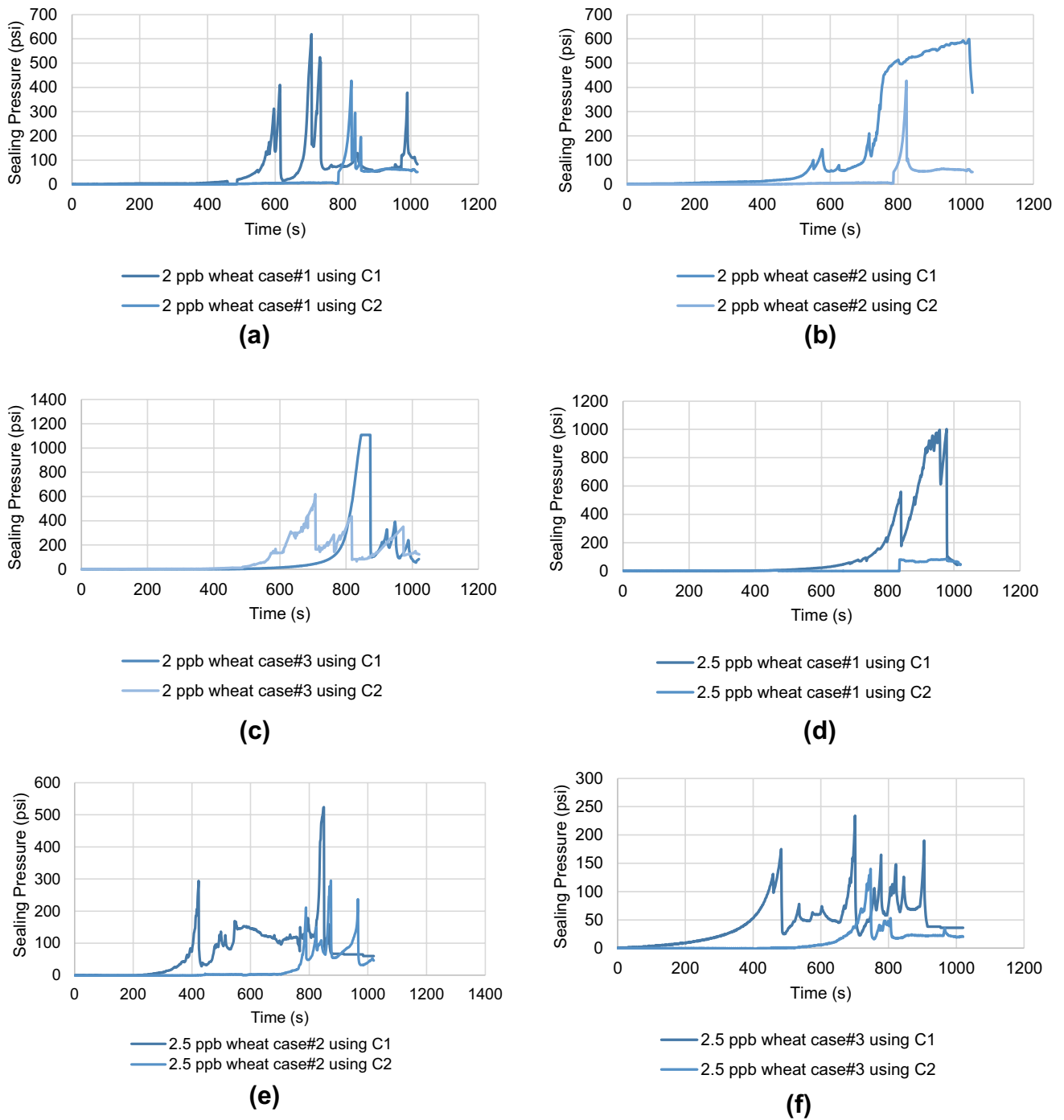


**Fig. 20** HPA Pressure versus Time plot for 2 & 2.5 ppb Wheat Straw showing maximum sealing pressure at different fracture widths, **a** case#1, **b** case#2, **c** case#3, **d** case#1, **e** case#2, **f** case#3

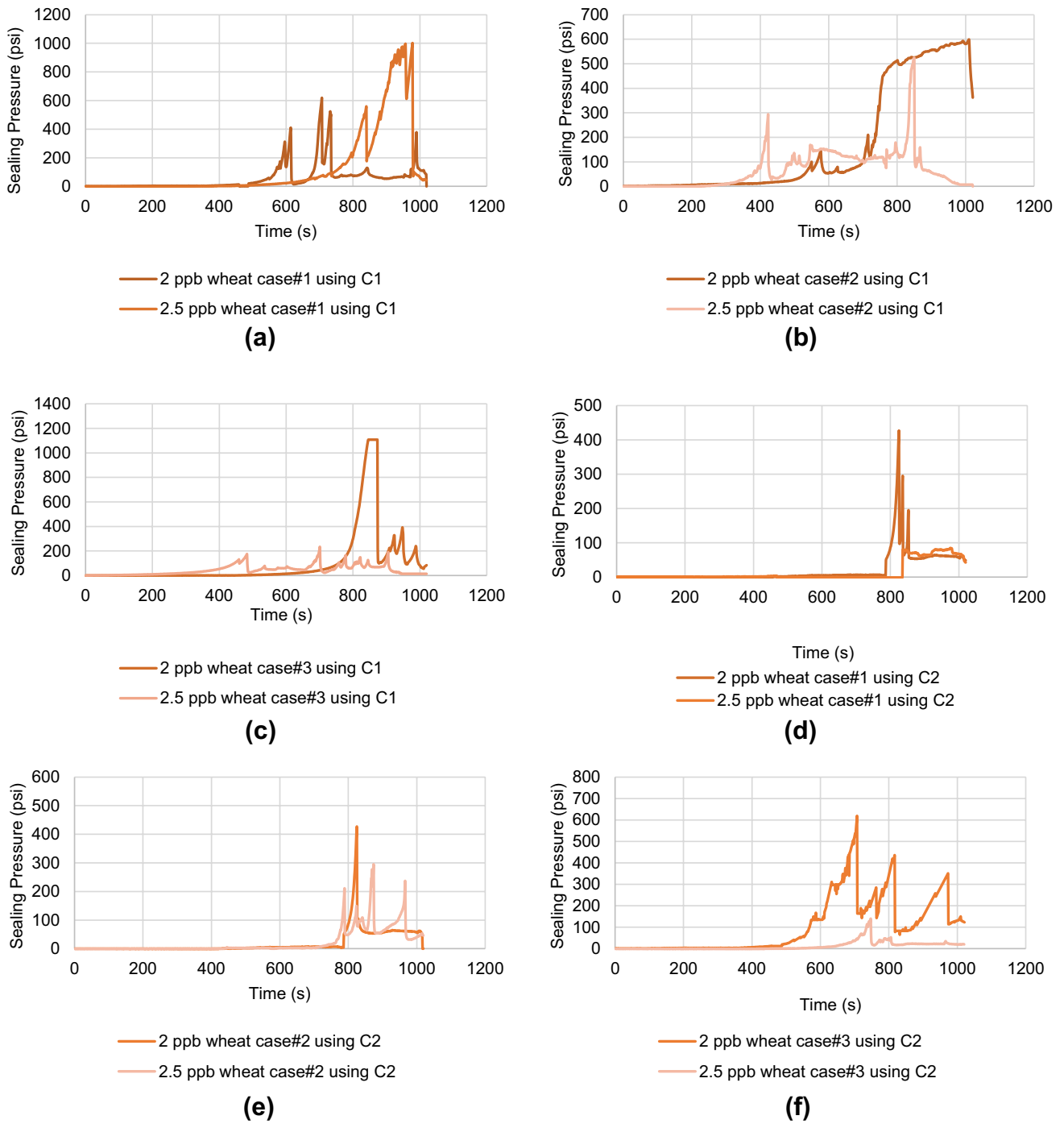


**Fig. 21** HPA Pressure versus Time plot for Wheat Straw showing maximum sealing pressure at different concentrations, **a** case#1, **b** case#2, **c** case#3, **d** case#1, **e** case#2, **f** case#3

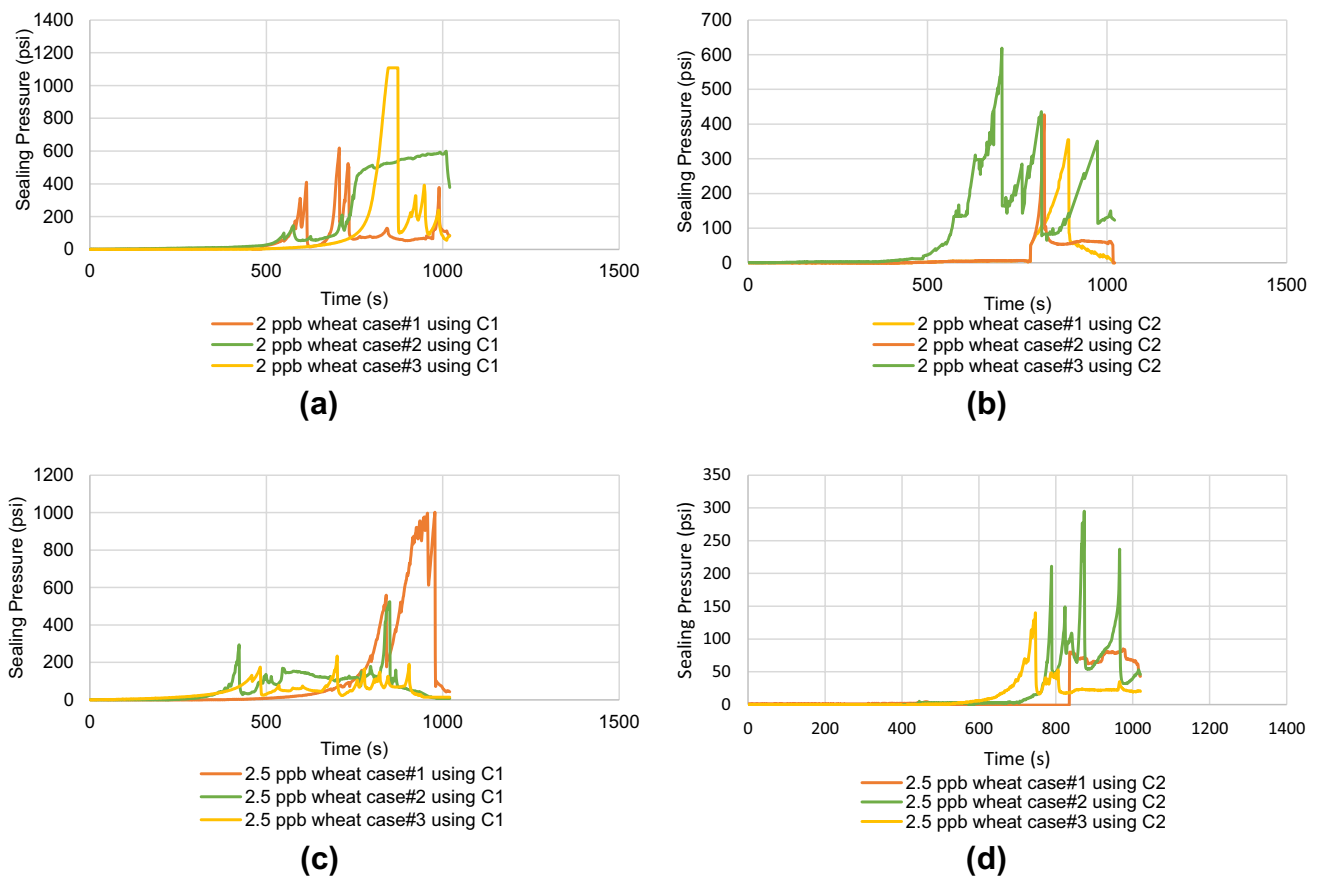


**Fig. 22** HPA Pressure versus Time plot for 2 & 2.5 ppb Wheat Straw showing maximum sealing pressure at different cases using C1 and C2

lar particles. This, in turn, considerably impacts the maximum sealing pressure.

**Mixture of LCMs** This section selected the best particle size and concentration of each LCM and combined them. Table 11 provides the best combination of them. The LPA fluid loss results are listed in Table 12 for LCM combinations. The HPA testing results are summarized in Table 13. As shown in Table 12, in the case of using a combination of LCMs, the amount of LPA fluid loss is much less, particularly for Mica, Oak Shell, and Wheat Straw mixture, which have the least value in LPA fluid loss. Table 13 suggests that Mica, Oak Shell, and Wheat Straw mixture have the least and most value in HPA fluid loss and maximum sealing pressure, respectively; therefore, it has the best performance among other LCMs mixtures.

Figure 29a shows the maximum sealing pressure using 56 ppb Mica & Canes blend when tested at different fracture widths. A 8.7% decrease (2254 to 2058 psi) in the maximum sealing pressure for 56 ppb Mica

& Canes blend was observed when the fracture width was increased from 1 to 3 mm. Figure 29b shows the maximum sealing pressure using 56 ppb Mica & Oak Shell blend when tested at different fracture widths. A 9.2% decrease (2593 to 2354 psi) in the maximum sealing pressure for 56 ppb Mica & Oak Shell blend was observed when the fracture width was increased from 1 to 3 mm. Figure 29c shows the maximum sealing pressure using a 56 ppb Mica & Wheat Straw blend when tested at different fracture widths. A 10% decrease (2511 to 2258 psi) in the maximum sealing pressure for 56 ppb Mica & Oak Shell blend was observed when the fracture width was increased from 1 to 3 mm. Figure 29d shows the maximum sealing pressure using a 6 ppb Oak Shell & Canes blend when tested at different fracture widths.

An insignificantly increase (2096 to 2110 psi) in the maximum sealing pressure for the 6 ppb Oak Shell & Canes blend was observed when the fracture width was increased from 1 to 3 mm. Figure 29e shows the maximum sealing pressure using a 6 ppb Oak Shell & Wheat

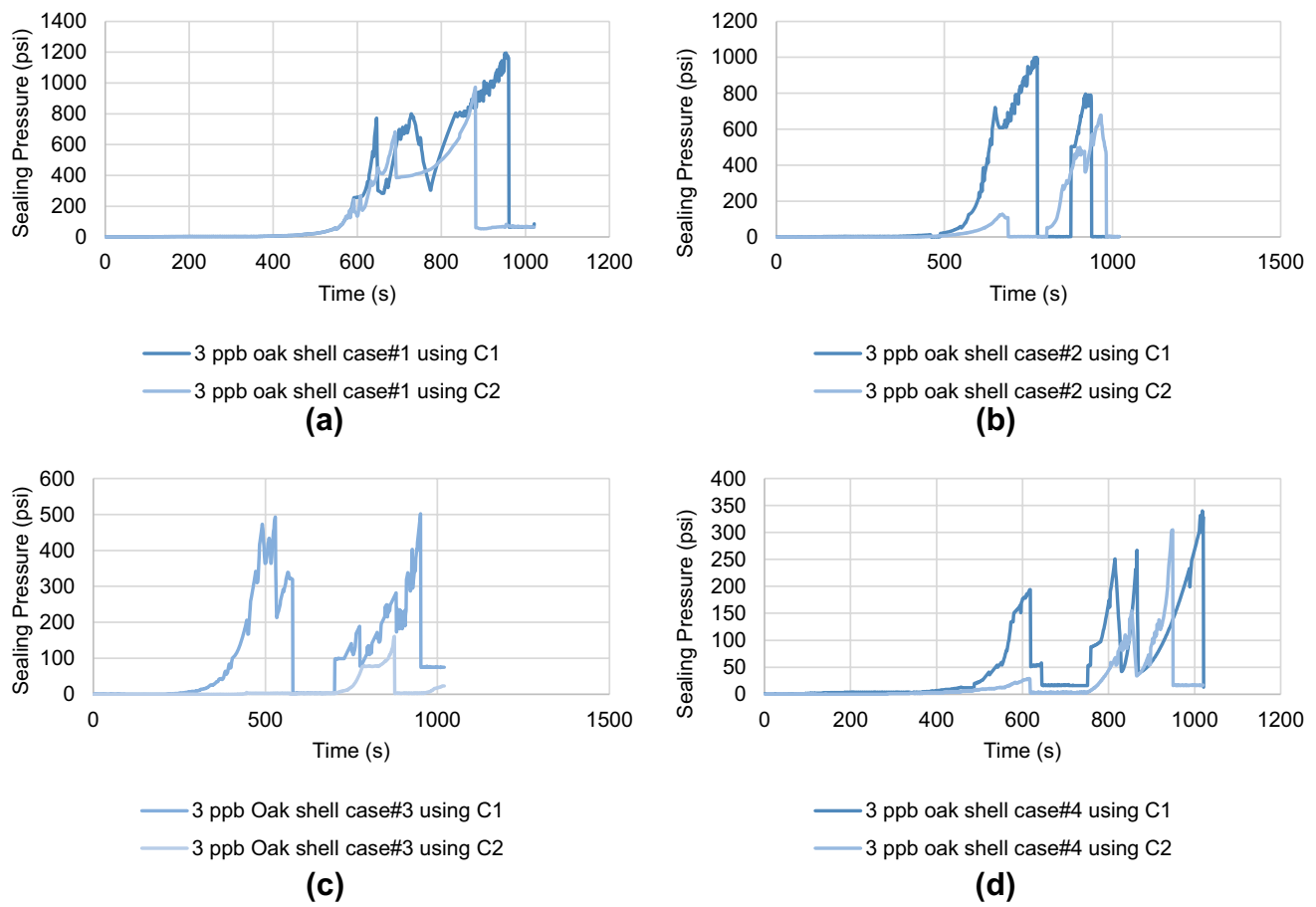


**Fig. 23** HPA Pressure vs. Time plot for 3 ppb Oak Shell showing maximum sealing pressure at different fracture widths, **a** case#1, **b** case#2, **c** case#3, **d** case#4

Straw blend when tested at different fracture widths. A 9.3% decrease (2740 to 2486 psi) in the maximum sealing pressure for 6 ppb Oak Shell & Wheat Straw blend was observed when the fracture width was increased from 1 to 3 mm.

Figure 29f shows the maximum sealing pressure using a 56 ppb Mica, Oak Shell & Wheat Straw blend when tested at different fracture widths. A 5% decrease (3026 to 2875 psi) in the maximum sealing pressure for 56 ppb Mica, Oak Shell & Wheat Straw blend was observed when the fracture width was increased from 1 to 3 mm. Figure 29 shows that if the combination of LCMs is used, increasing fracture width has no more effect on its performance.

**Results repeatability** To ensure the repeatability of the results, 50 ppb Mica case#1 and 6 ppb Oak Shells were

repeated for C1 and C2, shown in Fig. 30a–d. Mica and Oak Shells gave comparable results with an insignificant variation of 1% for C1 and 7% for C2, 3% for C1, and 4% for C2, respectively. Figure 30a–d illustrate that the conducted experiments are repeatable.

### Analysis of the experimental results and discussion

The fluid loss per cycle values from HPA tests showed a strong correlation with fluid loss values from LPA tests (these values are not equal, but their increasing or decreasing trend is similar). Some fluid losses per cycle values were significantly higher than the LPA values. This is due to the continuous injection of drilling fluid through a permeable seal that was not sealed well. The high seal permeability is due to larger LCM particles screening out at the fracture



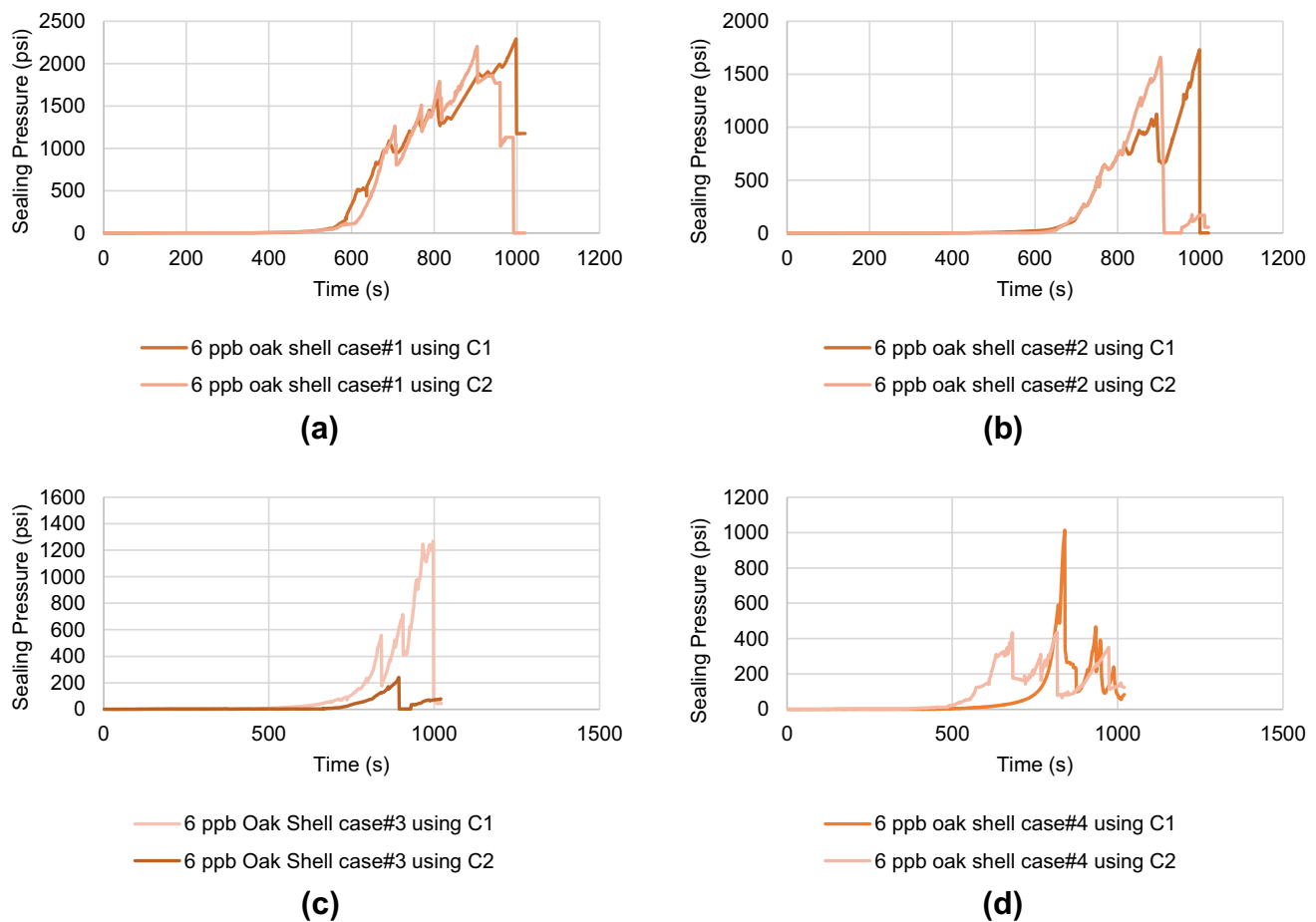


**Fig. 24** HPA Pressure vs. Time plot for 6 ppb Oak Shell showing maximum sealing pressure at different fracture widths, **a** case#1, **b** case#2, **c** case#3, **d** case#4

surface. This comparison also highlights the effect of higher LCM concentration on fluid loss. The comparison between fluid loss values from the LPA and the calculated average fluid loss per cycle from HPA using C1 and C2 is shown in Fig. 31a–b. To understand the effect of particle size distribution, the results were grouped in terms of the concentration and the fracture width (C1 and C2) shown in Fig. 32a–d.

The x-axis represents the four different LCMs in the four cases used in the tests, and the y-axis represents the measured fluid loss in ml. Figure 32a shows the particle size distribution (PSD) effect using low LCM concentration to seal a 1000-micron fracture. PSD has a huge influence on a fluid loss before forming the seal. The lowest fluid loss values were observed when case#1 formulation of Mica, case#3 formulation of Wheat Straw, case#1 formulation of Oak Shell, and case#1 formulation of Canes were used. The

fluid loss increased as the coarser particles increased in the blends. However, this was not the case when Wheat Straw was used due to optimum concentrations of coarse particles. The trend was slightly different when using high LCM concentration, as shown in Fig. 32b. In general, blends with a wide range of particle sizes exhibited the lowest fluid loss for all the LCMs except for Wheat Straw (Case#3). Even though increasing the concentration will reduce the fluid loss volume, a negative effect on the fluid loss occurred, as shown in Fig. 32b when case#4 for both Mica and Oak Shell, case#3 for Wheat Straw was used. When larger particles were the only particles within the blend, the fluid loss increased due to two factors; larger particles accumulated at the fracture face, creating a very permeable porous medium, and not having fine particles to fill the smaller pores between the larger particles.

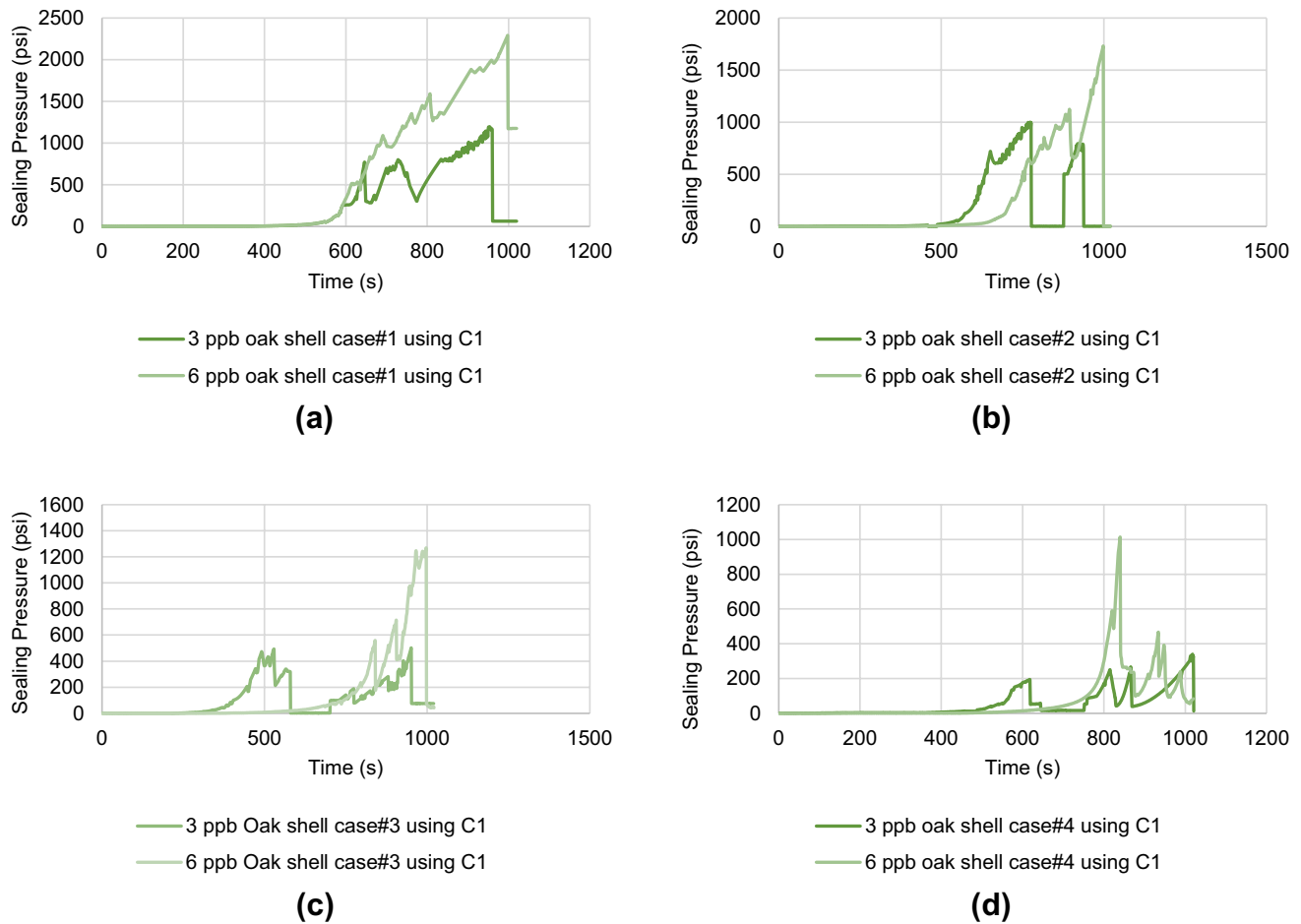


**Fig. 25** HPA Pressure versus Time plot for Oak Shell showing maximum sealing pressure at different concentrations, **a** case#1, **b** case#2, **c** case#3, **d** case#4

A significant increase in the fluid loss volume was observed when the fracture width was increased from 1 to 3 mm, as shown in Fig. 32c. The similarity in the observed trends suggests a strong relationship between PSD and sealing capability; therefore, an optimized PSD is required. Again, a significant reduction in the fluid loss was observed when using high LCM concentration, as shown in Fig. 32d. However, some cases exhibited the negative increased permeability effect mentioned above.

When the D50 particle size is less, the fracture width does not have a good performance, such as in case#3 of Oak Shell, while case#3 of Canes has the same characteristics but has a good performance, which is why these particles from 0.5 to 1 cm in length, and they can close the fracture. LPA results suggest that the largest particle size for a specific

fracture width is equal to or slightly larger than the anticipated fracture width. The overall performance of LCMs when used individually or in combinations in terms of the sealing pressures and average fluid loss per cycle is presented in Fig. 33a and b for each fracture width. The results are plotted and circled in groups as high to low performance. A 25 ppb Mica case#1, 50 ppb Mica case#1, 25 ppb Mica case#2, 6 ppb Oak Shell case#1, 6 ppb Canes case#1, 6 ppb Canes case#2, 56 ppb Mica & Canes, 56 ppb Mica & Oak Shell, 52 ppb Mica & Wheat Straw, 6 ppb Oak Shell & Canes, 6 ppb Oak Shell & Wheat Straw and 56 ppb Mica, Oak Shell & Wheat Straw (group a) performed the best in sealing 1 mm fracture width (see Fig. 33a).

Group b shows lower seal integrity with a relatively higher fluid loss value. The low performance of 2 ppb

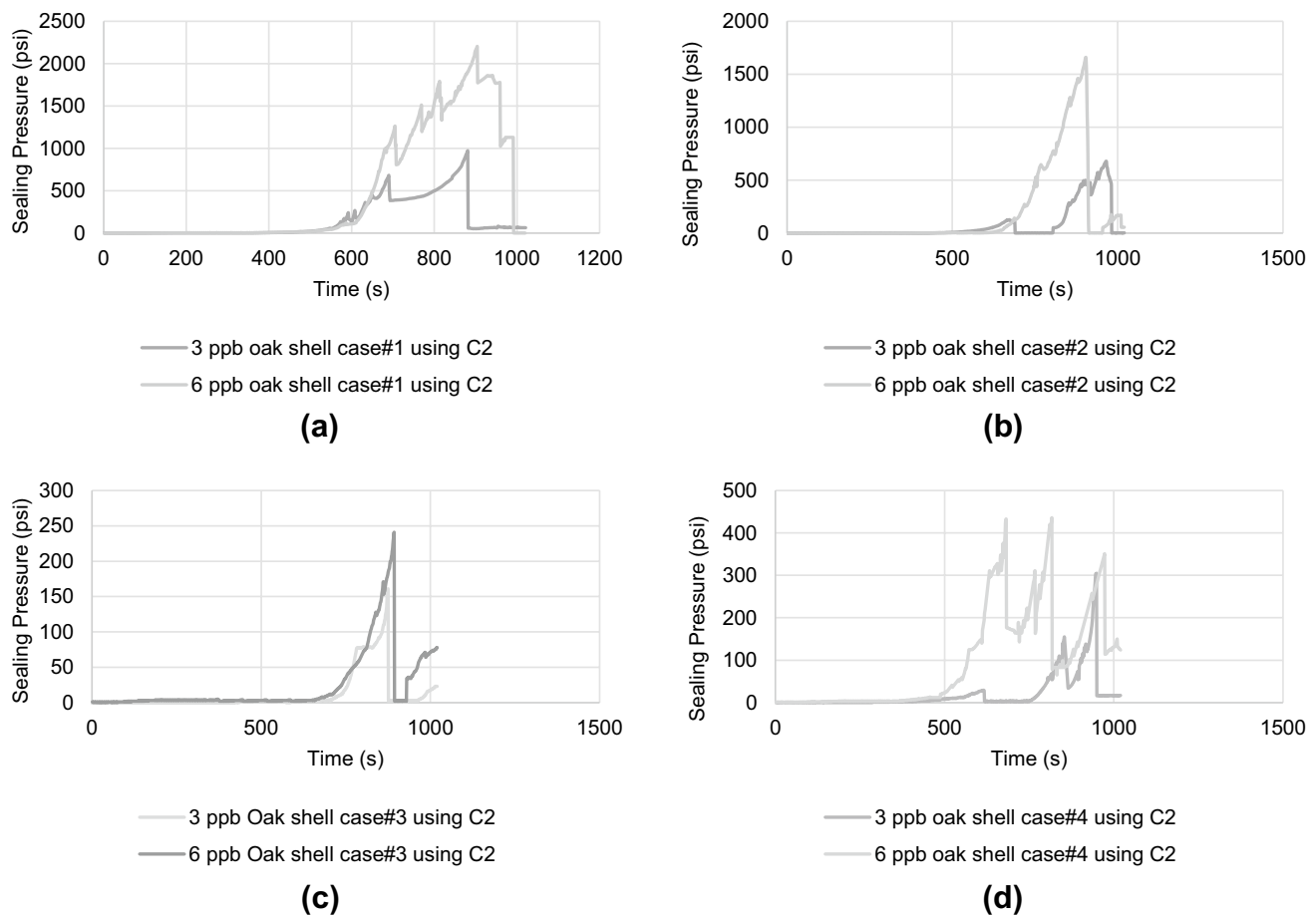


**Fig. 26** HPA Pressure versus Time plot for Oak Shell showing maximum sealing pressure at different concentrations, **a** case#1, **b** case#2, **c** case#3, **d** case#4

Wheat Straw blend case#1 is because Wheat Straw particles will have lower friction among themselves, which will add some sort of lubricity, and as a result, the formed seals will have lower integrity. Group c (6 ppb Oak Shell blend case#2) screened out at the fracture that it made only one pressure cycle and had much more fluid loss. When the same LCM and concentration were evaluated for a 3 mm fracture width (see Fig. 33b), blends of 25 ppb Mica, case#1, 25 ppb Mica, case#2, 50 ppb Mica, case#1, 50 ppb Mica, case#2, 6 ppb Oak Shell case#1, 6 ppb Canes case#1, 56 ppb Mica & Canes, 56 ppb Mica & Oak Shell, 52 ppb Mica & Wheat Straw, 6 ppb Oak Shell & Canes, 6 ppb Oak Shell & Wheat Straw and 56 ppb Mica, Oak Shell & Wheat Straw were able to seal the fracture with sealing pressures similar to those observed using C1 that are due to the wide range of PSD.

However, more fluid loss was observed, indicating that de-fluidization is required to seal wide fractures. When the Oak Shell and Mica were evaluated for wider fracture (C2) using the HPA, the sealing pressure using C2 for 6 ppb Oak Shell blend case#1 and 50 ppb Mica blend case#1 was relative to those observed using C1 but with a much higher fluid loss values. This shows that the increase in fracture width was not affected by Oak Shells and Mica blends.

Group b shows moderate sealing pressure and fluid loss value. High sealing pressure was observed for 6 ppb Oak Shell blend case#2 at very higher fluid loss values (group c) that de-fluidization was required to form a strong seal for fractures wider than 1 mm). To further analyze the data obtained, it was decided to use the following methodologies to extract more information. Normally, the maximum pressure observed has been reported. In addition to traditional

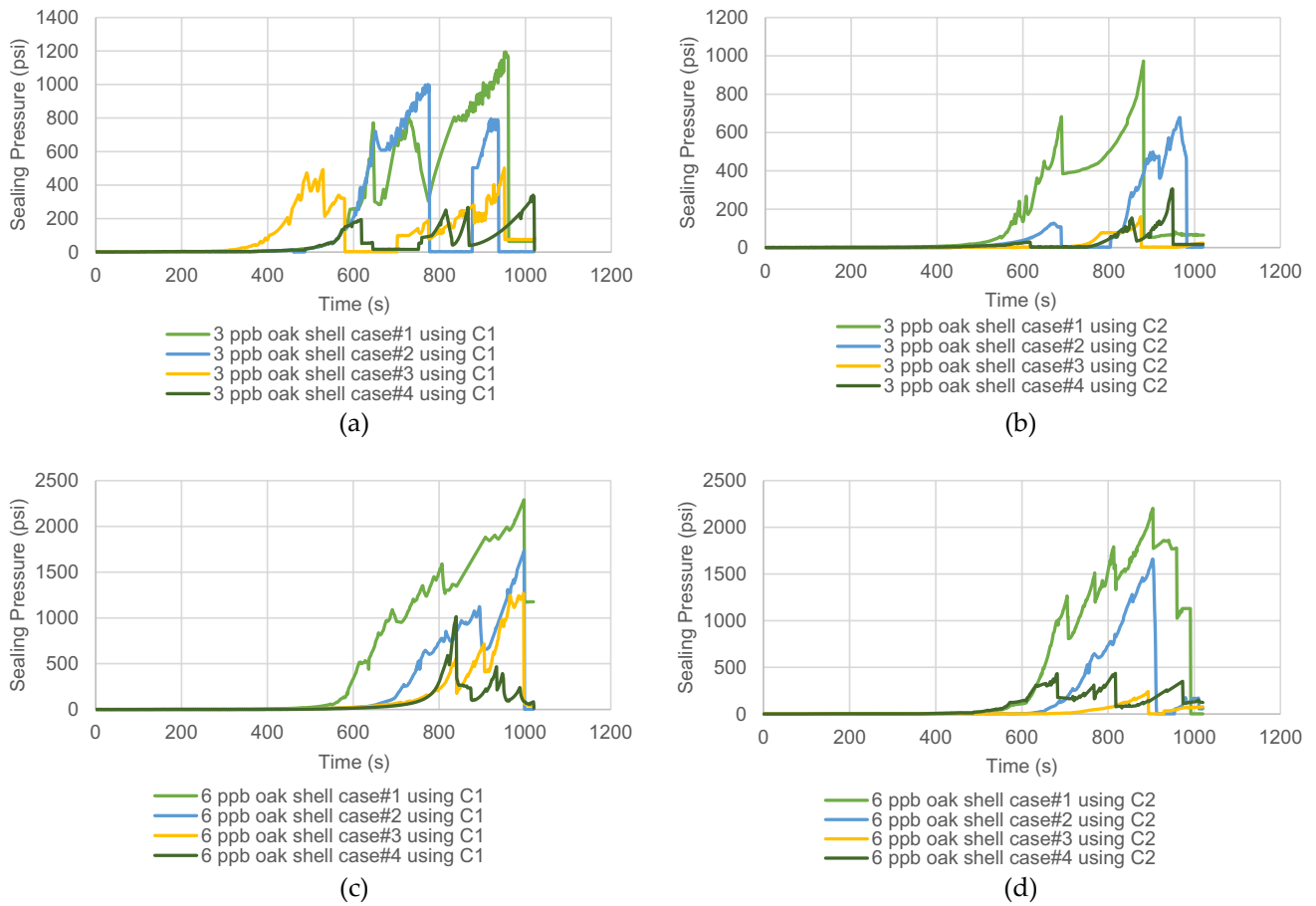


**Fig. 27** HPA Pressure versus Time plot for 3 & 6 ppb Oak shell showing maximum sealing pressure at different cases using C1 and C2

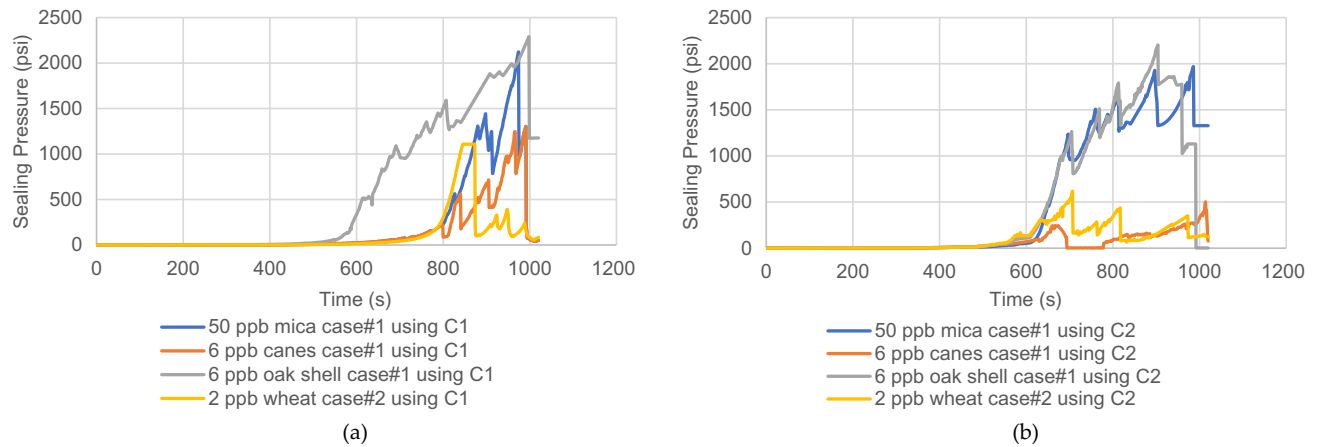


**Fig. 28** HPA Pressure vs. Time plot for Mica, Canes, Oak Shell, and Wheat Straw showing maximum sealing pressure at the best particle size and concentration using C1 & C2

**Table 11** LCM's concentration and PSD, when used in combinations

	D50 Micron	The weight percentage of total concentration, if used in combinations					
		Mica & Canes	Mica & Oak Shell	Mica & Wheat Straw	Oak Shell & Canes	Oak Shell & Wheat Straw	Mica, Oak Shell & Wheat Straw
Mica (M)	440	17.86	17.86	19.23	–	–	17.86
	1540	17.86	17.86	19.23	–	–	17.86
	1840	26.78	26.78	28.85	–	–	26.78
	3650	26.78	26.78	19.23	–	–	26.78
Wheat Straw (W)	6100	–	–	1.925	–	16.67	1.78
	1520	–	–	1.925	–	16.67	1.78
Oak Shell (OS)	740	–	3.57	–	16.67	22.23	2.38
	1660	–	3.57	–	16.67	22.23	2.38
	3700	–	3.57	–	16.67	22.23	2.38
Canes (C)	530	3.57	–				
	1570	3.57	–				
	3300	3.57	–				

**Table 12** LPA fluid loss results in (ml) for LCM combinations

LCM type	Concentration (ppb)	Fracture width (micron)	
		1000 (C1)	3000 (C2)
LPA fluid loss (ml)			
Mica & Canes	50 6	2	14
Mica & Oak Shell	50 6	1	12
Mica & Wheat Straw	50 2	1	12
Oak Shell & Canes	3 3	2	13
Oak Shell & Wheat Straw	4 2	0	11
Mica, Oak Shell & Wheat Straw	50 4 2	0	9

**Table 13** Summary of HPA testing results for LCM combinations

Test	Cell	LCM type	Concentration (ppb)	LPA fluid loss (ml)	Maximum sealing pressure (psi)	Total fluid loss (ml)	Average fluid loss (ml/cycle)
61	C1	M & C	56	2	2254	7	1.00
62		M & OS	56	1	2593	5	1.25
63		M & W	52	1	2511	7	1.17
64		OS & C	6	2	2096	12	2
65		OS & W	6	0	2740	4	0.8
66	C2	M, OS & M	56	0	3026	3	0.43
67		M & C	56	14	2058	87	12.43
68		M & OS	56	12	2354	77	15.40
69		M & W	52	12	2258	81	13.50
70		OS & C	6	13	2110	72	18.00
71		OS & W	6	11	2486	65	13.00
72		M, OS & M	56	9	2875	53	8.83

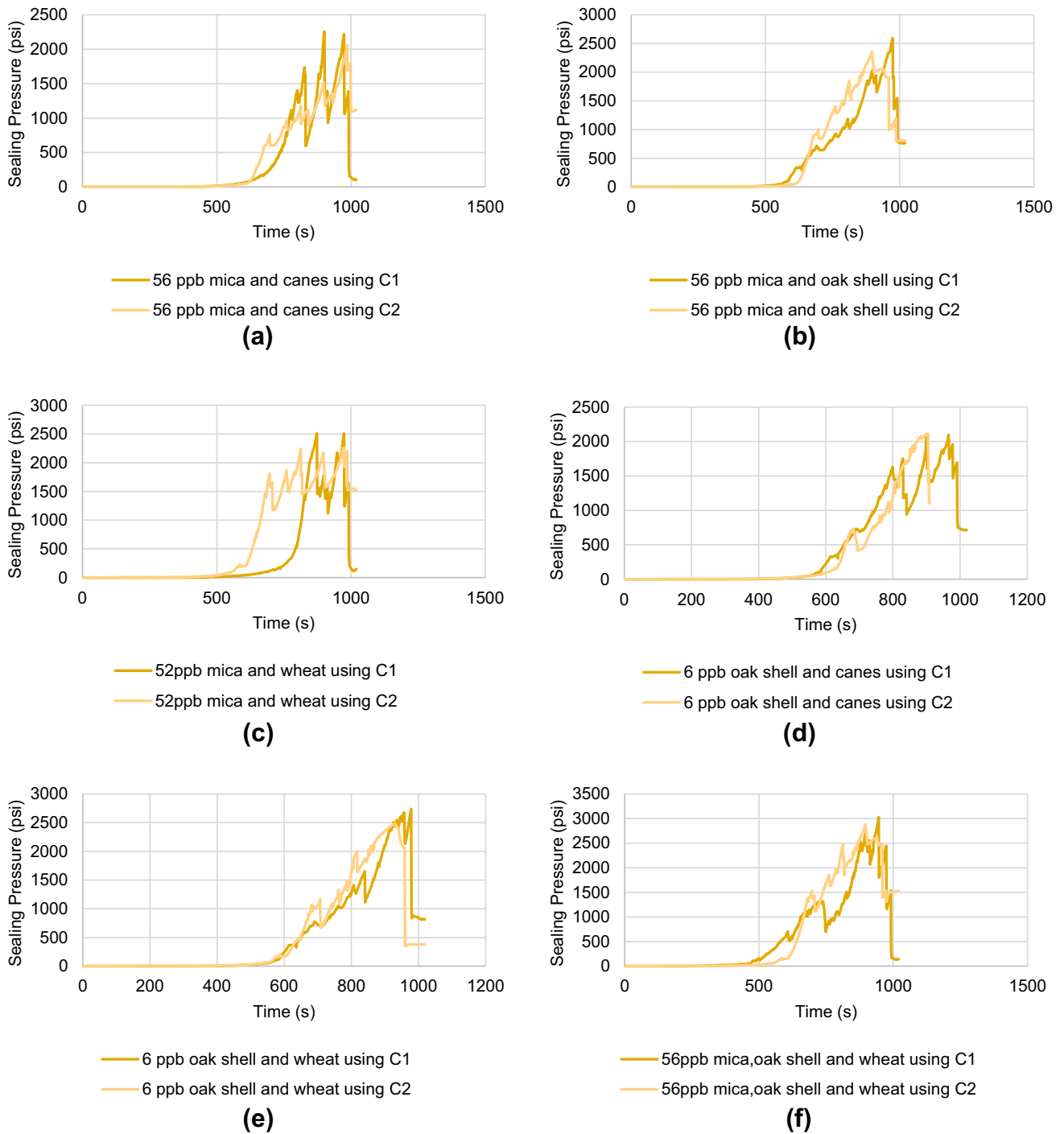


**Fig. 29** HPA Pressure vs. Time plot for the mixture of LCMs showing maximum sealing pressure at the best particle size and concentration and different fracture widths

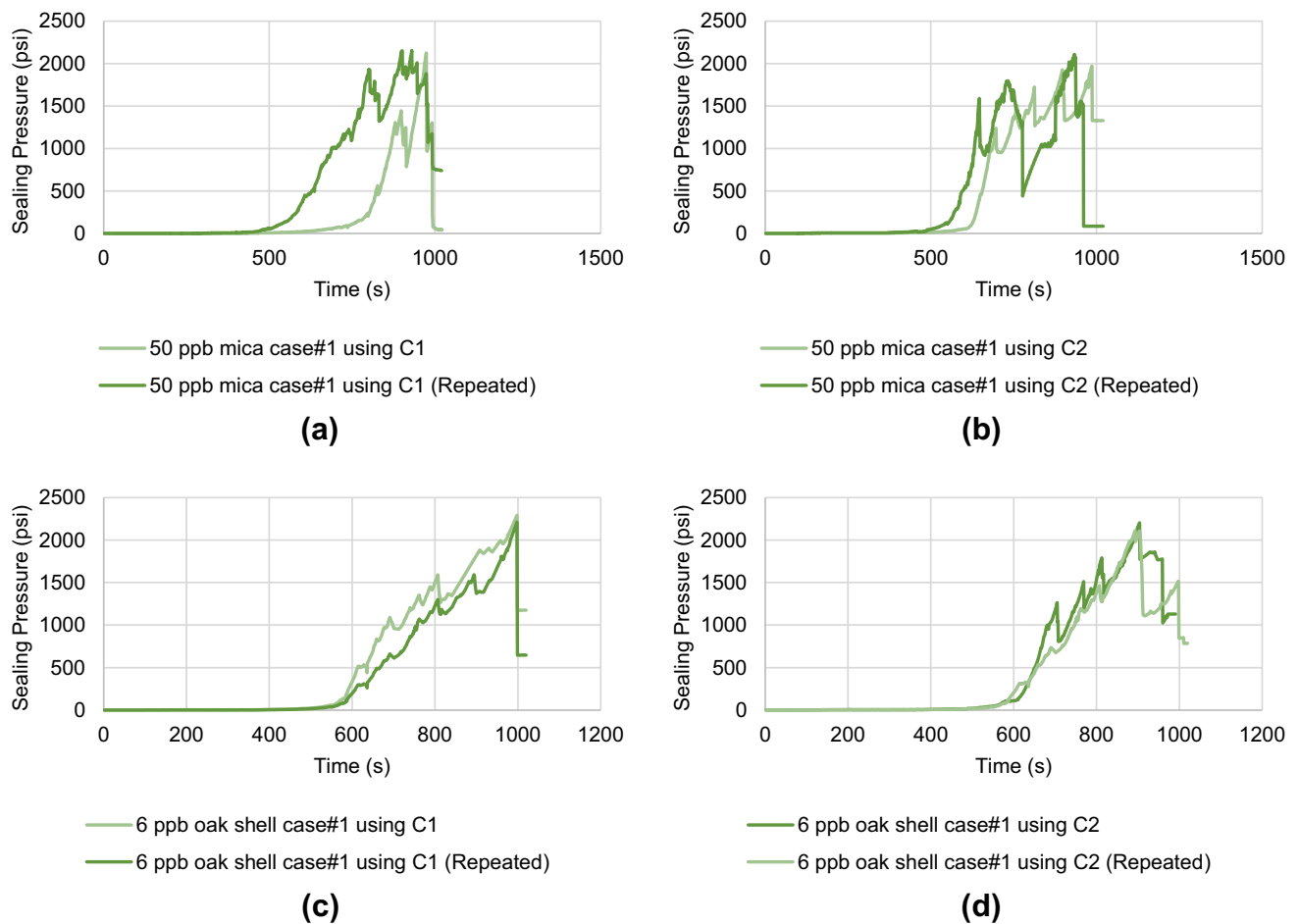


**Fig. 30** Repeated tests for Mica and Oak Shell using C1 and C2

parameters, other parameters are used (Mostafavi et al. 2011):

1. Maximum pressure in the cell ( $P_{\max}$ ). This parameter describes the maximum strength of the bridge during the experiment: the maximum pressure on the HPA pressure vs. the time plot.
2. The average pressure in the cell ( $P_{\text{avg}}$ ). This parameter refers to the mean pressure value during the experiment, the average data pressure on the HPA pressure vs. the time plot.
3. Average Peak Pressure in the cell ( $P_{\text{peak}}$ ). During the experiment, the peak pressure values show the strength of the formed bridges. The particles form bridges more than once during the experiment. The average peak pressure values show the average strength of the bridges.

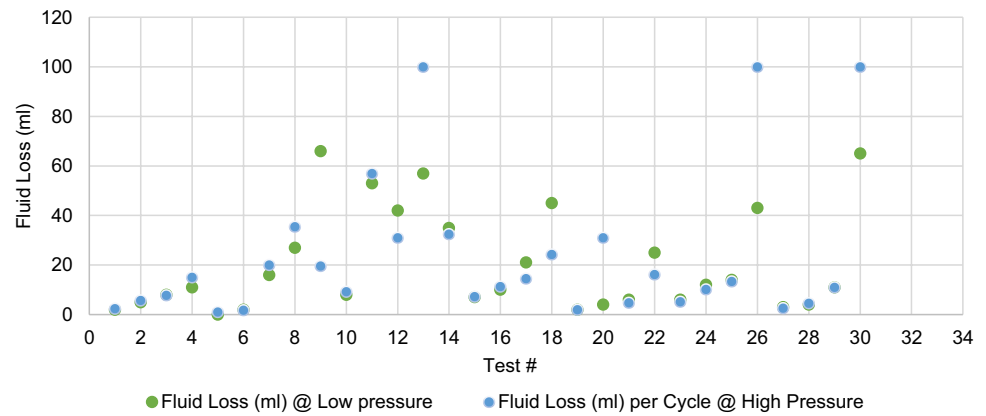
They are a reliable measure to analyze the sealing resistance and the average pressure of peak points on the HPA pressure vs. time plot. Mica is considered the base to compare pressure parameters, and other LCMs are measured. The performance of LCMs when used individually or in combinations in terms of the maximum sealing pressures, average pressure, and peak pressure is presented in Fig. 34a and b for each fracture width.

#### 4. 1000-Micron Fracture Width

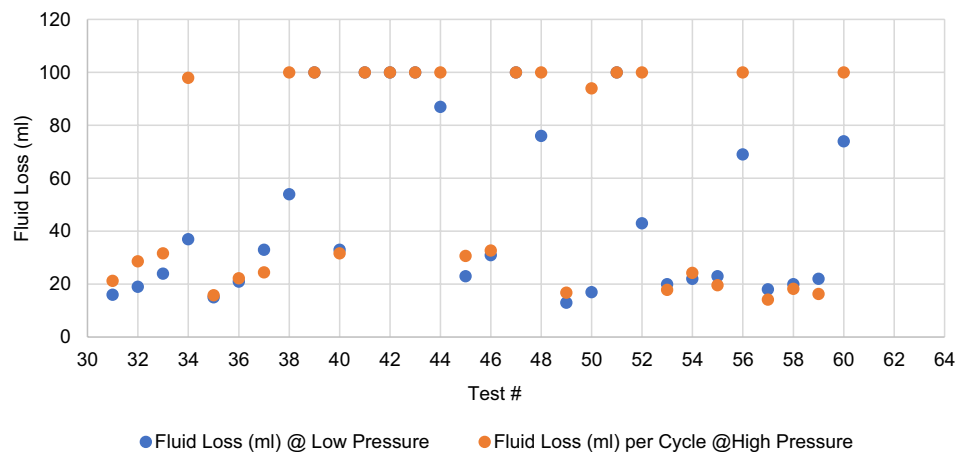
From the comparison of maximum pressure, average pressure, and average peak pressure, it was observed that in the case of 1000 micron, the bridging is initiated more frequently, tolerating more pressure, and with a higher maximum pressure when using the mixture of LCMs such as



**Fig. 31** Comparison between fluid loss values from the LPA and the calculated average fluid loss per cycle from HPA using C1 and C2



(a)



(b)

Mica & Canes, Mica & Oak Shell, Mica & Wheat Straw, Oak Shell & Canes, Oak Shell & Wheat Straw and Mica, Oak Shell & Wheat Straw. So the performance of the mixture of LCMs is excellent. Oak Shell reveals a slightly lower maximum pressure, higher average pressure, and higher average peak pressure. The data makes it possible to conclude that the Oak Shell behaves marginally better.

### B. 3000-Micron Fracture Width

The Canes graph shows that the average peak pressure is the same in both LCMs; average pressure slightly differs, whereas maximum pressure differs, higher in Mica. It is possible to conclude that Mica behaves slightly better. The maximum pressure, average pressure, and average peak pressure are lower in Wheat Straw, so the Wheat Straw

performance is lower. The same situation occurs in the test with 3000 micron, higher maximum pressure, higher average pressure, and higher average peak pressure when using the mixture of LCMs such as Mica & Canes, Mica & Oak Shell, Mica & Wheat Straw, Oak Shell & Canes, Oak Shell & Wheat Straw, and Mica, Oak Shell & Wheat Straw. Therefore, the performance of the mixture of LCMs is excellent. The Oak Shell graph shows that the average pressure is the same in both LCMs; the average peak pressure slightly differs, whereas the maximum pressure differs, higher in Oak Shells. It is possible to conclude that Mica behaves better. The maximum pressure, average pressure, and average peak pressure are remarkably lower in Canes and Wheat Straw, so the performances of Canes and Wheat Straw are lower.

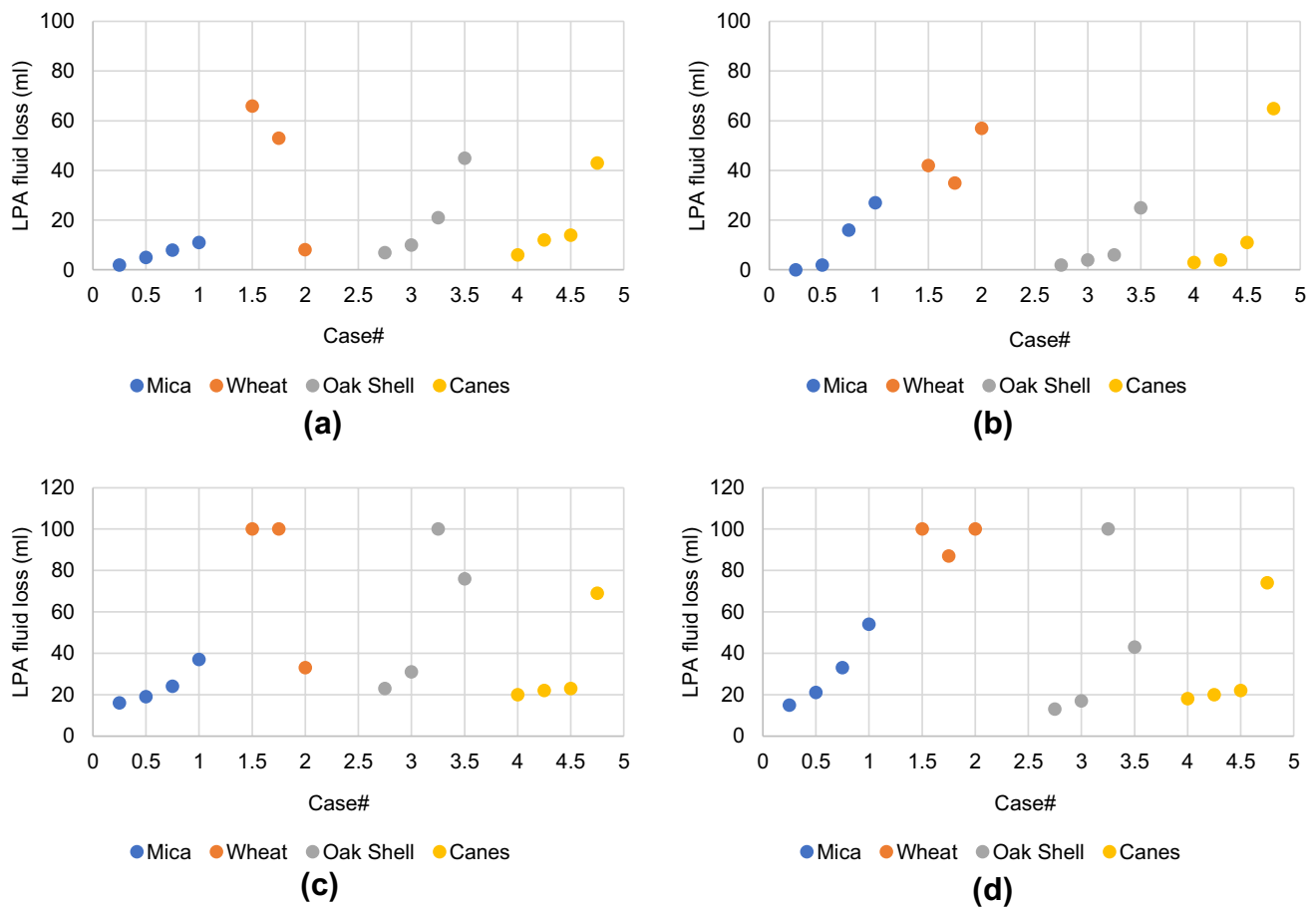


Fig. 32 The effect of PSD on fluid loss using C1 & C2 at high & low LCM concentration

## Prospects of this work

For future works, it is recommended that:

- Use cores from rocks to accurate simulation of fracture sealing.
- Use other lost circulation materials to investigate the capacity of fracture sealing, such as Walnut Shells and Oyster Shells.
- In this work, a fracture length of 50 mm was used. It is also necessary to investigate the effect of length on fracture sealing.
- All tests are done with water-based drilling fluid; use oil-based drilling fluid for more investigation.
- Investigate the effect of temperature on lost circulation.
- Investigate the effect of the injection rate on lost circulation.

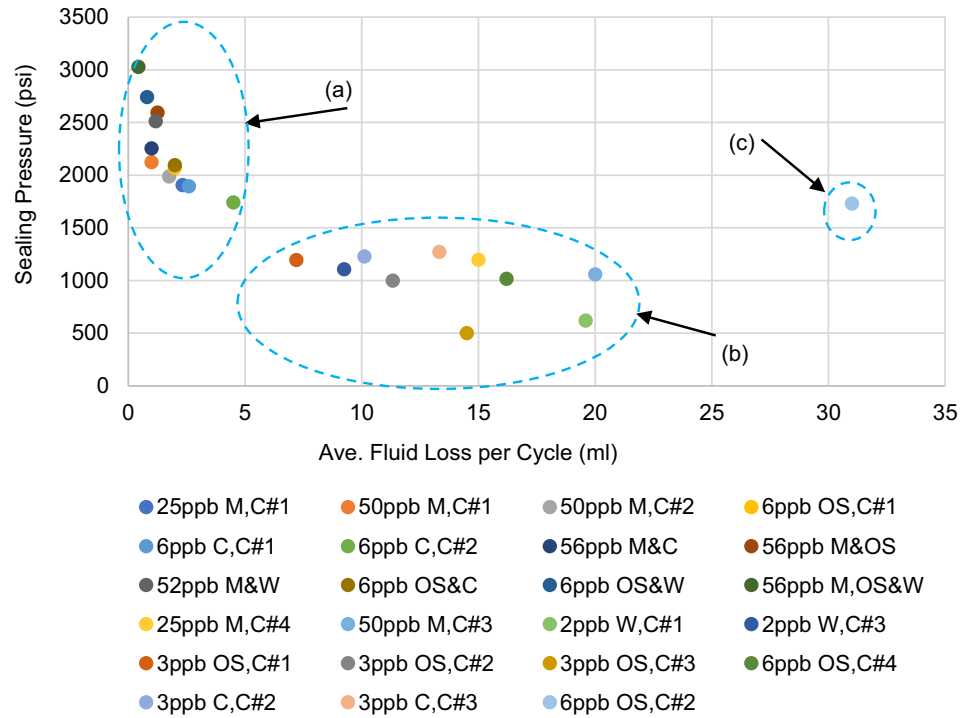
- Investigate the effect of fluid properties on lost circulation.
- Establishing the rheological model for basic mud samples with LCMs.
- Establishing zeta potential for the basic mud samples and with LCMs.

## Conclusions

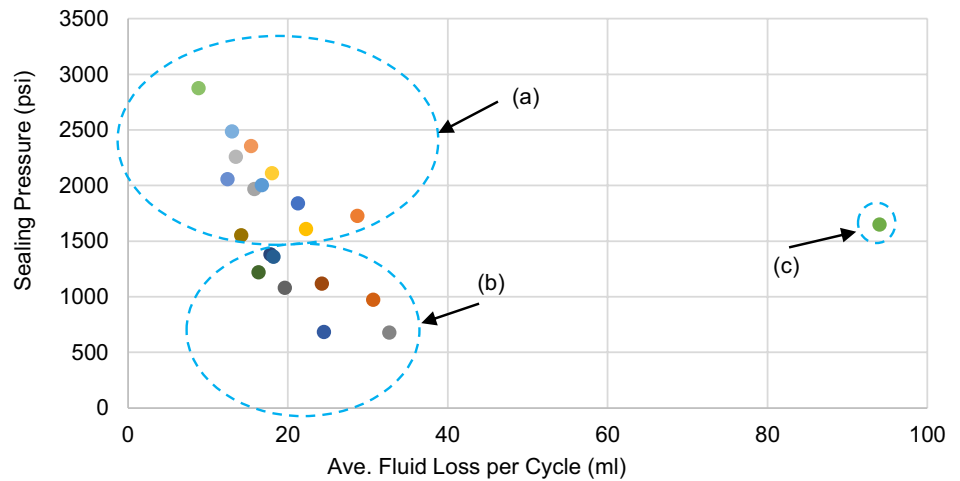
From the testing results, the following was concluded:

1. Fracture widths (1000 and 3000 microns) are predicted based on well-log data and adaptation of existing models in the desired oil field.
2. As a result, it has been investigated that judging by the maximum pressure, average pressure, average peak pres-

**Fig. 33** Overall Performance of LCM using 1 mm & 2 mm cell (C1 & C2). **a** Higher sealing pressures were observed at lower fluid loss values < 5 ml at small fracture widths. **b** Screen out at the fracture mouth caused higher fluid loss. **c** Lower seal integrity with relatively higher fluid loss value for one test. **d** High sealing pressures in conjunction with low fluid loss values due to the wide range of PSD. **e** Moderate sealing pressure and fluid loss values. **f** High sealing pressures were observed for OS at very higher fluid loss values (De-fluidization was required to form a strong seal for fractures wider than 1 mm)



(a)



(b)

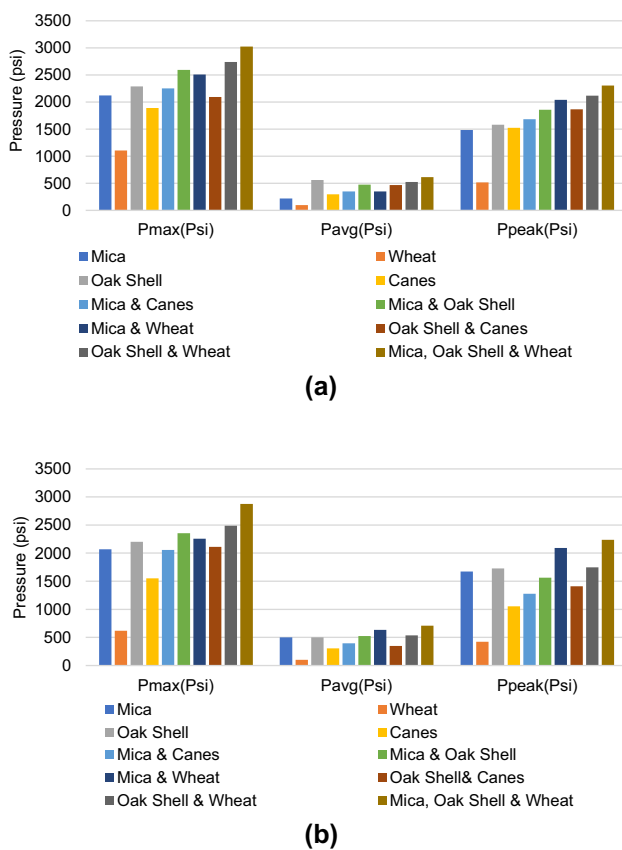


**Fig. 34** Pressure parameters with 1000 & 3000 micron cells and all LCMs

sure, and fluid loss value, when LCM was used individually, the performance of an Oak Shell and Mica blends were the best in the tests with 1 mm and 3 mm cells with a concentration of 6 and 50 ppb, respectively. When LCM was used in combination, the performance of all mixtures of LCM was better than LCM when used individually, and the performance of the mixture of Mica, Oak Shell, and Wheat Straw was the best with a concentration of 56 ppb.

- When the Oak Shell and Mica blends were evaluated for wider fracture (C2) using the HPA, the sealing pressure using C2 was relatively similar to those observed using C1. It shows that the increase in fracture width is not affected by Oak Shells and Mica blends.
- In general, it was observed that higher LCM concentration gave better results; however, there is a maximum critical concentration at which LCM will not penetrate the fracture, and no tight seal will be formed.
- The results show that LCM with irregularity in particle shape, such as Oak Shell blend, can seal wide fractures

and maintain good seal integrity when used individually or in combination with other LCM.

- The results suggest that the largest particle size for a specific fracture width is equal to or slightly larger than the anticipated fracture width. On the other hand, when large particles are the only particles within the blend, the fluid loss increases, so fine particles are required to fill the smaller pores among the larger particles. Therefore, using vastly distributed particles would give more relevant results.
- The results reveal a strong relationship between fluid loss and maximum sealing pressure, *i.e.*, the lower fluid loss gave higher maximum sealing pressure.
- The calculated fluid loss per cycle from the HPA for conventional LCM is directly related to observed LPA fluid loss.
- Due to the abundance and low cost of these materials in the study area, they can be used to ensure successful plugging.

**Funding** The authors received no financial support for this article's research, authorship, and publication.

#### Declaration

**Conflict of interest** The corresponding author states that there is no conflict of interest on behalf of all authors.

**Open Access** This article is licensed under a Creative Commons Attribution 4.0 International License, which permits use, sharing, adaptation, distribution and reproduction in any medium or format, as long as you give appropriate credit to the original author(s) and the source, provide a link to the Creative Commons licence, and indicate if changes were made. The images or other third party material in this article are included in the article's Creative Commons licence, unless indicated otherwise in a credit line to the material. If material is not included in the article's Creative Commons licence and your intended use is not permitted by statutory regulation or exceeds the permitted use, you will need to obtain permission directly from the copyright holder. To view a copy of this licence, visit <http://creativecommons.org/licenses/by/4.0/>.

## References

- AlAwad M (2022) A new approach for understanding the mechanism of wellbore strengthening theory. *J King Saud Univ Eng Sci* 34(1):67–76. <https://doi.org/10.1016/j.jksues.2020.07.015>
- Alsaba M, Nygaard R, Saasen A, Nes O (2016) Experimental investigation of fracture width limitations of granular lost circulation treatments. *J Pet Explor Prod Technol* 6:593–603. <https://doi.org/10.1007/s13202-015-0225-3>
- Alsaba M (2016) Investigation of lost circulation materials impact on fracture gradient. Doctoral thesis. Missouri University of science and technology

- Alsaba M, Nygaard R (2014) Laboratory evaluation of sealing wide fractures using conventional lost circulation materials. In: SPE annual technical conference and exhibition, Amsterdam, The Netherlands, 27–29 October 2014. SPE-170576-MS
- Al-saba MT, Nygaard R, Saasen A, Nes O-M (2014a) Laboratory evaluation of sealing wide fractures using conventional lost circulation materials. In: SPE annual technical conference and exhibition, Society of Petroleum Engineers
- Al-saba MT, Nygaard R, Saasen A, Nes O-M (2014b) Lost circulation materials capability of sealing wide fractures. In: SPE deepwater drilling and completions conference, Society of Petroleum Engineers
- Arshad U, Jain B, Pardawalla H, Gupta N, Meyer A (2014) Engineered fiber-based loss circulation control pills to successfully combat severe loss circulation challenges during drilling and casing cementing in northern Pakistan. Paper SPE 169343, presented at the SPE Latin American and Caribbean petroleum engineering conference. Society of Petroleum Engineers, Maracaibo, Venezuela
- Cook J, Growcock F, Guo Q, Hodder M, van Oort E (2012) Stabilizing the wellbore to prevent lost circulation. *Oilfield Rev* 23(4):26–35
- Cook J, Guo Q, Way P, Bailey L, Friedheim J (2016) The role of filtercake in wellbore strengthening. Paper IADC/SPE 17899-MS, presented in IADC/SPE drilling conference and exhibition, Fort Worth, TX, USA
- Ezeakacha CP, Salehi S, Hayatdavoudi A (2017) Experimental study of drilling fluid's filtration and mud cake evolution in sandstone formations. *ASME J Energy Resour Technol* 139(2):022912
- Ghalambor A, Salehi S, Shahri M, Karimi M (2014) Integrated workflow for loss circulation prediction. Paper-SPE 168123-MS, presented in SPE international symposium and exhibition for formation damage and control, Lafayette, LA, USA
- Jeennakorn M, Nygaard R, Nes O, Saasen A (2017) Testing conditions make a difference when testing LCM. *J Nat Gas Sci Eng* 46:375–386. <https://doi.org/10.1016/j.jngse.2017.08.003>
- Kefi S, Lee JC, Shindgikar ND, Brunet-Cambus C, Vidick B, Diaz NI (2010) Optimizing in four steps composite lost-circulation pills without knowing loss zone width. In: IADC/SPE Asia pacific drilling technology conference and exhibition, Society of Petroleum Engineers
- Kumar A, Savari S, Whitfill D, Jamison DE (2010) Wellbore strengthening: the less-studied properties of lost-circulation materials. In: SPE annual technical conference and exhibition, Society of Petroleum Engineers
- Mansour A, Dahi Taleghani A, Salehi S, Li G, Ezeakacha C (2019) Smart lost circulation materials for productive zones. *J Pet Explor Prod Technol* 9:281–296. <https://doi.org/10.1007/s13202-018-0458-z>
- Mansour AK, Taleghani D (2018) Smart loss circulation materials for drilling highly fractured zones. In: SPE/IADC middle east drilling technology conference and exhibition, Abu Dhabi, UAE. Paper Number: SPE-189413-MS. <https://doi.org/10.2118/189413-MS>
- Mostafavi V, Hareland G, Belayneh M, Aadnoy B (2011) Experimental and mechanistic modeling of fracture sealing resistance with respect to fluid and fracture properties. In: 45th US rock mechanics/geomechanics symposium, American Rock Mechanics Association
- Restrepo A, Osorio G, Duarte JE, Lopera Castro SH, Hernandez J (2010) LCM plugging effect on producing formations during drilling naturally fractured sandstone reservoirs. In: SPE international symposium and exhibition on formation damage control, Society of Petroleum Engineers
- Savari, SL, Whitfill D (2019) Managing lost circulation in highly fractured, vugular formations: engineering the LCM design and application. In: Abu Dhabi international petroleum exhibition and conference, Abu Dhabi, UAE, SPE-197186-MS. <https://doi.org/10.2118/197186-MS>
- Whitfill D (2008) Lost circulation material selection, particle size distribution and fracture modeling with fracture simulation software. In: IADC/SPE Asia pacific drilling technology conference and exhibition, Society of Petroleum Engineers
- Xu Ch, Kang Y, You L, You Zh (2017) Lost-circulation control for formation-damage prevention in naturally fractured reservoir: mathematical model and experimental study. *SPE J* 22(05):1654–1670. <https://doi.org/10.2118/182266-PA>
- Yang M, Ch Y (2020) Investigation of LCM soaking process on fracture plugging for fluid loss remediation and formation damage control. *J Nat Gas Sci Eng*. <https://doi.org/10.1016/j.jngse.2020.103444>

**Publisher's Note** Springer Nature remains neutral with regard to jurisdictional claims in published maps and institutional affiliations.